Sedimentologika

Research article

Depositional model and sedimentation controls of a complex hybrid carbonate–siliciclastic ramp (Albian) – SW Campos Basin, Brazil

Francyne Bochi do Amarante[1*], Claiton Marlon dos Santos Scherer[2], Garibaldi Armelenti[1], Luiz Fernando De Ros[2], Renata Alvarenga[1], Juliano Kuchle[2], João Claudio Conceição[1], José Luis Alves[1], Luiz Landau[1]

[1] Department of Civil Engineering (COPPE), Rio de Janeiro Federal University (UFRJ), Rio de Janeiro, Brazil
[2] Geosciences Institute, Rio Grande do Sul Federal University (UFRGS), Porto Alegre, Brazil

*corresponding author: Francyne Bochi do Amarante (francyneb@gmail.com)

doi: 10.57035/journals/sdk.2024.e22.1535

Editors: Stéphane Bodin and Orla Bath Enright
Reviewers: Two anonymous reviewers
Copyediting, layout and production: Romain Vaucher, Gabriel Bertolini and Elizabeth Mahon

Submitted: 16.03.2024
Accepted: 17.10.2024
Published: 29.11.2024

Abstract | Hybrid deposits form from the interaction between carbonate deposition and coeval siliciclastic input, influenced by spatial and temporal dynamics. This interaction occurs across various mixing scales, resulting in a high vertical and lateral lithological variability. Understanding this heterogeneity is crucial for comprehending and modelling hybrid reservoirs. The Albian succession of the SE Brazilian margin records the early evolution of the South Atlantic Ocean. In the Campos Basin, this interval is represented by a retrograding succession of shallow-marine carbonates (Quissamã Formation) overlain by deep marine calcilutites and shales. We use cored wells, petrographic thin sections and geophysical logs to detail the Albian in the SW Campos Basin, to characterize its depositional model and stratigraphical succession. We identified four facies associations that define different parts of a hybrid carbonate–siliciclastic ramp: carbonate shoal (subdivided into shallower and deeper portions), hybrid carbonate-siliciclastic shoal, and coastal environment. Carbonate shoals are composed of calcarenites and calcirudites with oolites, oncolites, peloids, bioclasts and intraclasts. Hybrid shoals also present calcarenites and calcirudites but include a significant siliciclastic fraction. Coastal environments are dominantly composed of hybrid arenites, locally dolomitized. Carbonate-siliciclastic mixing occurs at different scales: compositional mixing at bed scale, and strata mixing at lithofacies and stratigraphic scales. This sediment mixture results from the interaction between waves, currents, base-level variation cycles, and salt tectonics. Isolith maps of siliciclastic and carbonate facies of the Quissamã Formation reveal four NE-trending shoals aligned on a NW-SE trend. Chronostratigraphic analysis indicates that the shoals were non-contemporary, with the most distal shoal forming earlier, indicating a retrograding, backstepping pattern for the Albian in the Campos Basin.

Resumo | Depósitos híbridos se formam a partir da interação entre a deposição carbonática e o aporte siliciclástico coevo, influenciados por dinâmicas espaciais e temporais. Essa interação ocorre em diferentes escalas, resultando em uma alta variabilidade litológica vertical e lateral. Compreender essa heterogeneidade é essencial para interpretar e modelar reservatórios híbridos. A sucessão Albiana da margem sudeste brasileira registra o início da evolução do Oceano Atlântico Sul. Na Bacia de Campos, esse intervalo é representado por uma sucessão retrogradante de carbonatos marinhos rasos (Formação Quissamã) sobreposta por calcilutitos e folhelhos de ambiente marinho profundo. Utilizamos testemunhos de poços, lâminas petrográficas e perfis geofísicos para detalhar o intervalo Albiano no sudoeste da Bacia de Campos, com o objetivo de caracterizar seu modelo deposicional e sucessão estratigráfica. Identificamos quatro associações de fácies que definem diferentes partes de uma rampa híbrida carbonática-siliciclástica: banco carbonático (subdividido em porções mais rasas e mais profundas), banco híbrido carbonático-siliciclástico e ambiente costeiro. Os bancos carbonáticos são compostos por calcarenitos e calcirruditos contendo ooides, oncoides, pelóides, bioclastos e intraclastos. Os bancos híbridos também apresentam calcarenitos e calcirruditos, mas incluem uma fração siliciclástica significativa. Ambientes costeiros são predominantemente compostos por arenitos híbridos, localmente dolomitizados. A interação entre componentes carbonáticos e siliciclásticos ocorre em diferentes escalas: mistura composicional em nível de camada e mistura de estratos nas escalas de litofácies e estratigráfica. Essa dinâmica sedimentar resulta da interação entre ondas, correntes, ciclos de variação do nível de base e tectônica salina. Mapas de isólitas das fácies siliciclásticas e carbonáticas da Formação Quissamã revelam quatro bancos com orientação NE, alinhados em um trend NW-SE. Análises cronoestratigráficas indicam que os bancos não eram contemporâneos, com

o banco mais distal se formando primeiro, evidenciando um padrão retrogradante e de recuo para o Albiano na Bacia de Campos.

Lay summary | This study investigates the interaction between carbonate and siliciclastic sediments in the Campos Basin, SE Brazil, during the Albian geological age, as the South Atlantic Ocean was forming. The mixing of these constituents creates diverse rock layers that characterize hybrid reservoirs. By analyzing well data, rock samples, and geophysical logs, we describe the Albian rock layers and identified distinct lithological associations that define different parts of a hybrid carbonate–siliciclastic ramp depositional environment: carbonate shoal, hybrid shoal and coastal setting. Our study indicates that this depositional environment was shaped by ocean currents, waves, and the tectonic movement of the underlying salt layers. Our findings also reveal that the carbonate shoals developed in stages, moving closer to the coast over time. This research enhances our understanding of ancient hybrid sedimentary environments and their influence on natural resources, paving the way for better exploration strategies.

Keywords: Macaé Group, Quissamã Formation, Búzios Member, Carbonate reservoir, Mixed sediments.

1. Introduction

Hybrid or mixed carbonate–siliciclastic systems refer to depositional settings where sedimentation includes both extrabasinal (e.g., terrigenous) and intrabasinal (autochthonous to parautochthonous) constituents (Zuffa, 1980; Mount, 1984). The mixing of these two types of constituents depends heavily on the processes responsible for producing and depositing different types of carbonate grains (skeletal and non-skeletal), as well as the processes supplying siliciclastic detritus to the basins (e.g., river discharge in a shallow-marine area; Zeller et al., 2015; Schwarz et al., 2016). There are several works on the characterization of hybrid deposits (among others, Tirsgaard, 1996; Amorosi & Zuffa, 2011; Betzler et al., 2011; Braga et al., 2012; Chiarella et al., 2016; Moretti et al., 2016; Rossi et al., 2017), but very few studies have explored the characteristics and controls of hybrid systems in which the contribution from non-skeletal carbonates is dominant (Gischler & Lomando, 2005; Michel et al., 2011; Schwarz et al., 2018).

Hybrid deposits hold significant importance in hydrocarbon exploration (McNeill et al., 2004). These hybrid deposits exhibit lateral and vertical heterogeneities, characterized by the presence of carbonate–siliciclastic layers, which form baffles and barriers significantly impacting flow behavior (Chiarella et al., 2017). Understanding the type and scale of carbonate–siliciclastic mixing across hybrid systems, and identifying the processes responsible for their formation, is crucial for accurate reservoir modeling and hydrocarbon exploration.

Marginal basins offshore SE Brazil are widely known for their significant economic value in hydrocarbon exploration, exploiting diverse tectono-stratigraphic settings such as syn-rift Neocomian basalts, post-rift Albian calcarenites, and early Miocene siliciclastic turbidites (e.g., Abelha & Petersohn., 2018; Bruhn at al., 2003). The Albian succession in these passive margin basins records the early development of the South Atlantic Ocean (i.e., post-rift or drift phase). In the Campos Basin this interval is represented by the Macaé Group that consists of a retrograding succession of shallow-marine carbonates (Quissamã Formation) overlain by deep marine calcilutites and shales (Outeiro Formation; Winter et al., 2007). The central area of the basin presents numerous oil fields producing from Albian carbonates of the Macaé Group (e.g., Carozzi et al., 1983; Guardado et al., 1989; Bruhn at al., 2003). Consequently, research on the Albian interval in the Campos Basin has concentrated on the central area, where the succession is interpreted as a carbonate ramp (e.g., Carozzi & Falkenhein, 1985; Guardado et al., 1989; Favoreto et al., 2015; Rebelo et al., 2021). The SW Campos Basin remains understudied, with our research revealing it to be a hybrid carbonate-siliciclastic ramp with mainly non-skeletal carbonates.

In this study, we integrate petrographic, sedimentological and geophysical data (mainly gamma-ray logs) to analyse the paleoenvironmental evolution of the Albian interval of SW Campos Basin. We identify 14 lithofacies, grouped into 4 facies associations: carbonate shoal – shallow portion, carbonate shoal – deeper portion, hybrid (carbonate/siliciclastic) shoal and coastal environment, defining a hybrid carbonate–siliciclastic ramp. We then discuss facies succession, and the primary factors influencing sediment distribution, focusing on the interplay between carbonate and siliciclastic components and facies.

2. Geological context

The Campos Basin, situated on the SE Brazilian margin offshore from the states of Espírito Santo and Rio de Janeiro, spans approximately 115,000 km² (Figure 1; Guardado et al., 1989; Winter et al., 2007). Its formation and development are intricately tied to the fragmentation of the Gondwana Supercontinent, ultimately resulting in the opening of the South Atlantic Ocean during the Late Jurassic to Early Cretaceous period (Szatmari, 2000).
In terms of stratigraphy, the Campos Basin can be divided into three distinct tectono-sedimentary units or mega-sequences: rift, sag, and passive margin (Guardado et al., 1989; Winter et al., 2007). Early rifting is characterized by

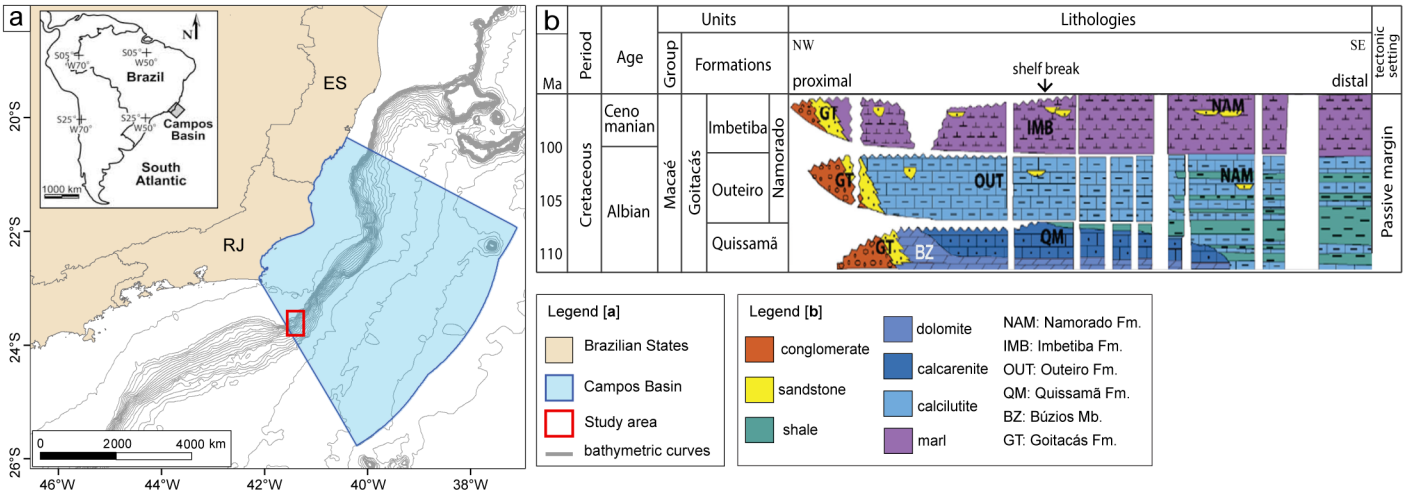

Figure 1 | (A) Regional map showing the location of Campos Basin and our study area polygon; abbreviations: RJ - Rio de Janeiro State, and ES - Espírito Santo State. (B) Simplified stratigraphic chart of the Albian – Cenomanian of Campos Basin (redrawn from Winter et al., 2007).

intense volcanism dated c. 122 to 134 million years ago (Mizusaki et al., 1998). Sedimentation in the initial tectono-sedimentary phase (rift, Barremian – Early Aptian) consists of continental lacustrine deposits (Winter et al., 2007). Rift tectonics generated normal faults, mainly NE-SW oriented, that bound horsts and grabens (Chang et al., 1992; Guardado et al., 2000).

The subsequent sag mega-sequence commenced in the late Aptian with the transition of mechanical subsidence induced by basement-involved normal faulting to a slower thermal subsidence driven by cooling and lithospheric contraction (Guardado et al., 1989; Amarante et al., 2023). The sedimentary succession within the sag mega-sequence of the Campos Basin comprises clastic sediments near the shoreline, and microbial carbonates in the basinward areas, overlain by a thick layer of evaporites (Dias et al., 1987).

The passive margin mega-sequence registers a rapid marine transgression during the Late Cretaceous linked to the initiation of basinal drift. Shallow-water carbonate platforms developed in the Albian, subsequently covered by pelagic and hemipelagic shale deposits and turbidites (Chang et al., 1992). Thermal subsidence concentrated near the location of continental breakup, which caused the basin to tilt to the SE, inducing gravity gliding and salt tectonics of the Aptian evaporites (Quirk et al., 2012), which define distinct structural domains of deformation (Amarante et al., 2021).

The open marine sedimentary succession of the Campos Basin initiated during the sag tectono-sequence with the deposition of carbonates of the Macaé Group (Albian – Cenomanian). This group comprises the Goitacás, Quissamã, Outeiro, Imbetiba, and Namorado formations. The Goitacás Formation comprises proximal clastic sediments of coastal environments, including alluvial fans, deltas and fan deltas (Winter et al., 2007). The Quissamã Formation primarily consists of packstones and grainstones composed of ooids, peloids, oncoids, and bioclasts, deposited within a NE-oriented shoal system (Guardado et al., 1989). These carbonates were deposited in a shallow neritic environment with a homoclinal carbonate ramp morphology, under moderate to high energy (Dias et al., 1990). The lower carbonates of the Quissamã Formation, directly overlaying the evaporites, are dolomitized and constitute the Búzios Member. The overlying Outeiro Formation comprises intercalations of calcilutites, marlstones, and shales, with sandstone bodies of the Namorado Formation, originating from turbidite flows (Castro & Picolini, 2016). The upper unit of the Macaé Group is the Imbetiba Formation, characterized by marlstones and calcilutites. Both the Outeiro and Imbetiba formations were deposited in deep marine environments (Winter et al., 2007). Overlying the Macaé Group is the Campos Group, which records a marine transgression during the Late Cretaceous, followed by a marine regression. This group is characterized by pelagic and hemipelagic prograding sediments and turbidite deposits (Winter et al., 2007).

3. Database and methodology

The database of this study consists of 30 boreholes that contain petrophysical logs (e.g., sonic travel time, bulk density, and gamma ray), stratigraphic (i.e., age) and lithology data (Figure 2). Out of the 30 boreholes, 5 contain core of the Quissamã Formation (Albian), totaling 200 m and 475 thin sections.

We logged the 200 m of core on a 1:50 scale. The delimitation of lithofacies was based on granulometric, textural and compositional parameters, and the presence of sedimentary structures. The facies codes of carbonate rocks consist of the abbreviation resulting from rock classification based on the dominant grain size (sensu Grabau, 1904 and Bramkamp & Powers, 1958) (CA = calcarenite; CR = calcirudite), followed by the main constituent (O = oncolytic; OO = oolitic; B = bioclastic). The letter "s" were added to carbonate facies with 10 – 30% of siliciclastic constituents, and the letter "d" to indicate

dolomitization. Hybrid carbonate-siliciclastic arenites (ARH) present more than 30% of siliciclastic components (Zuffa, 1980). Lowercase letters in parentheses represent sedimentary structures: l = low-angle cross-bedding; x = high-angle cross-bedding; w = wave-ripple cross-lamination; h = horizontal lamination. The individual lithofacies were grouped into facies associations, which correspond to a set of genetically related facies, and compose a sub-environment of a depositional system.

This study analyzed 475 thin sections from the Albian interval. To identify the porosity system, blue epoxy resin was applied, while staining with alizarin red and potassium ferrocyanide facilitated the identification of carbonate minerals (cf. Dickson, 1965). Digital photomicrographs were taken using the Zeiss AX10 Lab A1 microscope for qualitative and quantitative analysis of primary composition, diagenesis, and different pores. In selected thin sections, a modal count of 300 points was performed on each slide along transects, perpendicular to the rock structure and fabric. The Petroledge® software (De Ros et al., 2007) was used to recognize primary composition, diagenetic constituents, pore types, and textural aspects such as grain size, shape, structures, and overall rock structure.

Lithological and petrophysical data, primarily gamma-ray curves (when available), were employed to construct lateral correlation sections. These sections facilitated the examination of both vertical and lateral facies associations, enabling the interpretation of the spatial and temporal evolution within the Albian interval of the SW Campos Basin. Additionally, also based on the gamma-ray curves, we generated isolith maps showing the relative proportion between purely carbonate facies (i.e., CAO, CAOO, CRO), and hybrid facies (i.e., ARH, ARH(x), ARH(l)).

4. Results

4.1. Facies

Based on the description of c. 200 m and 475 thin sections of 5 cored wells (Figure 3), we identified 14 lithofacies, summarized in Table 1, and two post-depositional (i.e., diagenetic) facies, summarized in Table 2. Representative photos of the main lithofacies are shown in Figure 4. The petrographic analysis focused on three groups of lithofacies: dolomitized hybrid sandstones (present at the base of well 1-OGX-6-RJS, 3041.00 – 3010.00 m), hybrid sandstones and carbonates.

4.1.1. Petrographic characterization of the dolomitized hybrid arenites

Intensely dolomitized hybrid arenites (sensu Zuffa, 1980) are found at the basal portion of cored well 1-OGX-6, interbedded with dolosparites (Figure 3). They are grouped into the lithofacies ARH, ARH(x), ARH(l) and

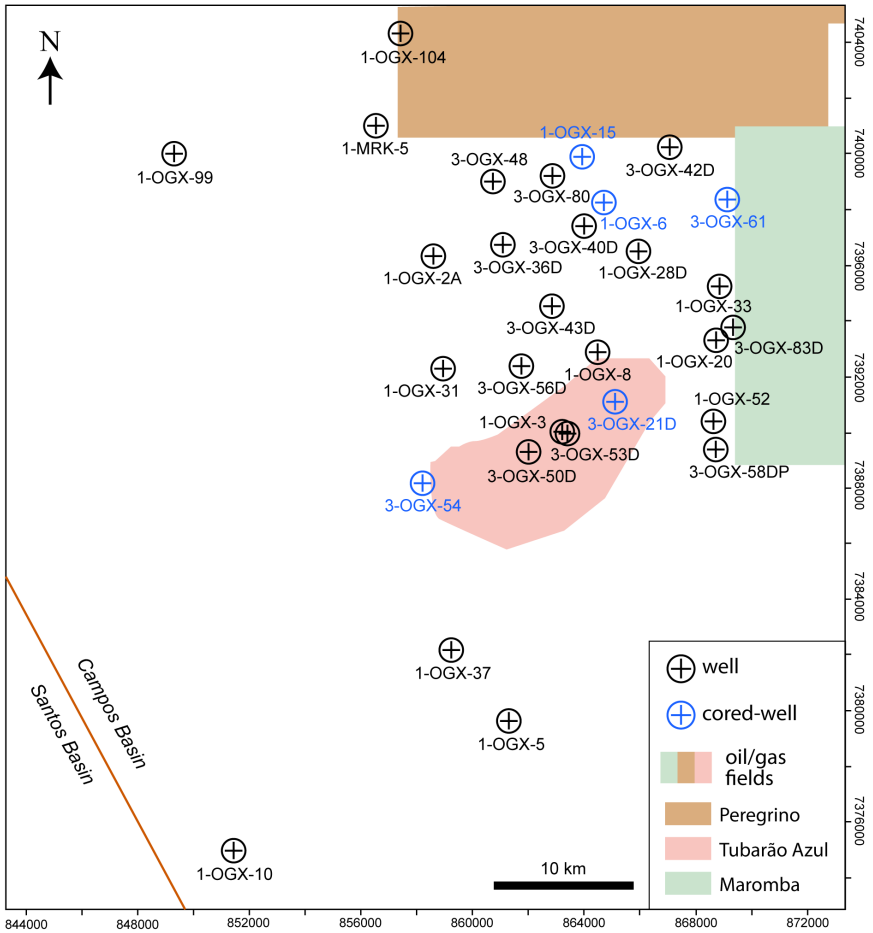

Figure 2 | Location of the 30 boreholes used in this study and the location of oil and gas fields in the region. Cored wells shown in Figure 3 are shown in blue.

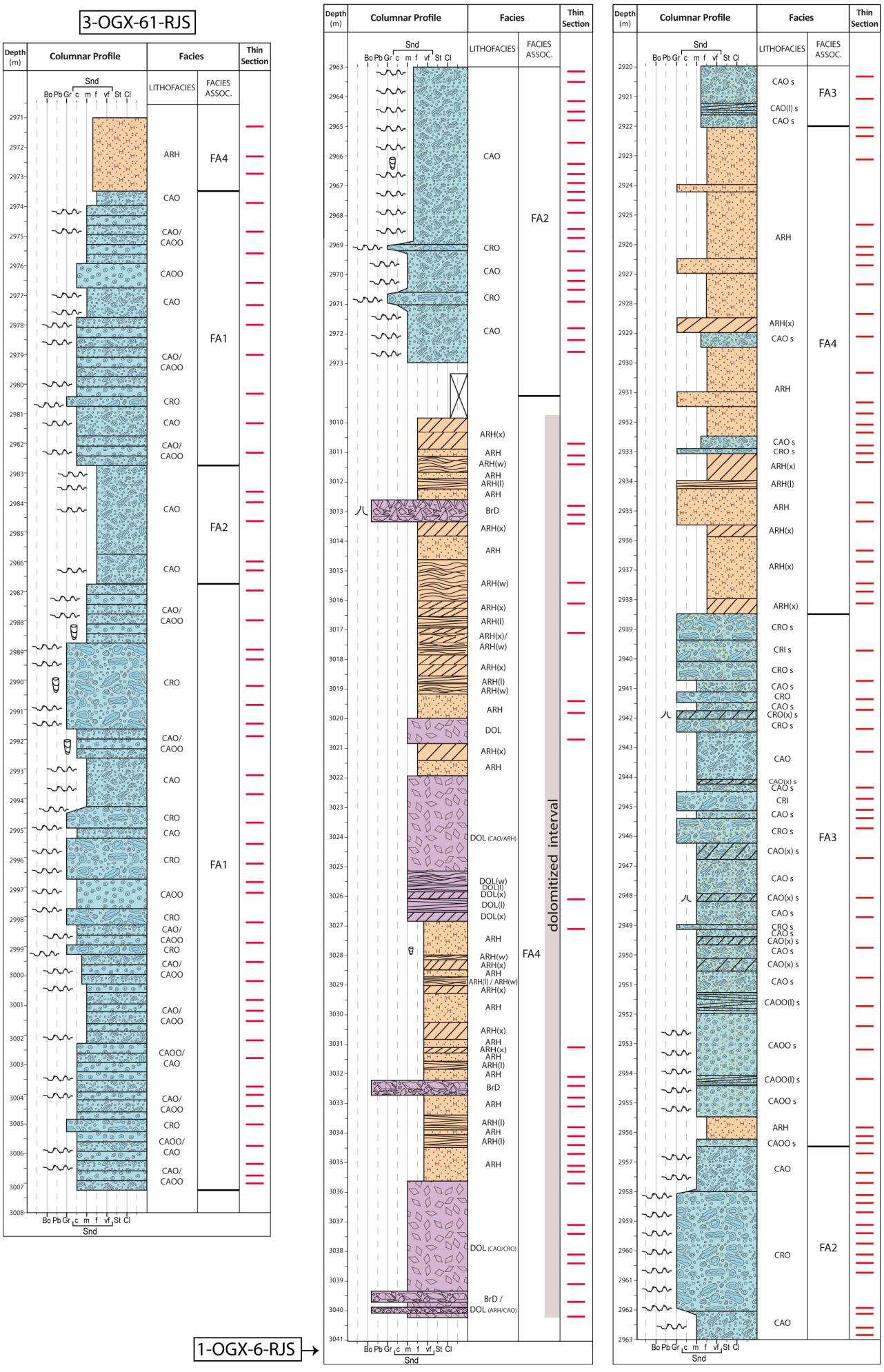

Figure 3 | Columnar profiles of the cored wells, with the interpreted facies and lithofacies, and depth of the thin sections; the map in the bottom of the figure shows the location of the wells. See Tables 1 and 2 for lithofacies codes, and Table 5 for facies associations codes.

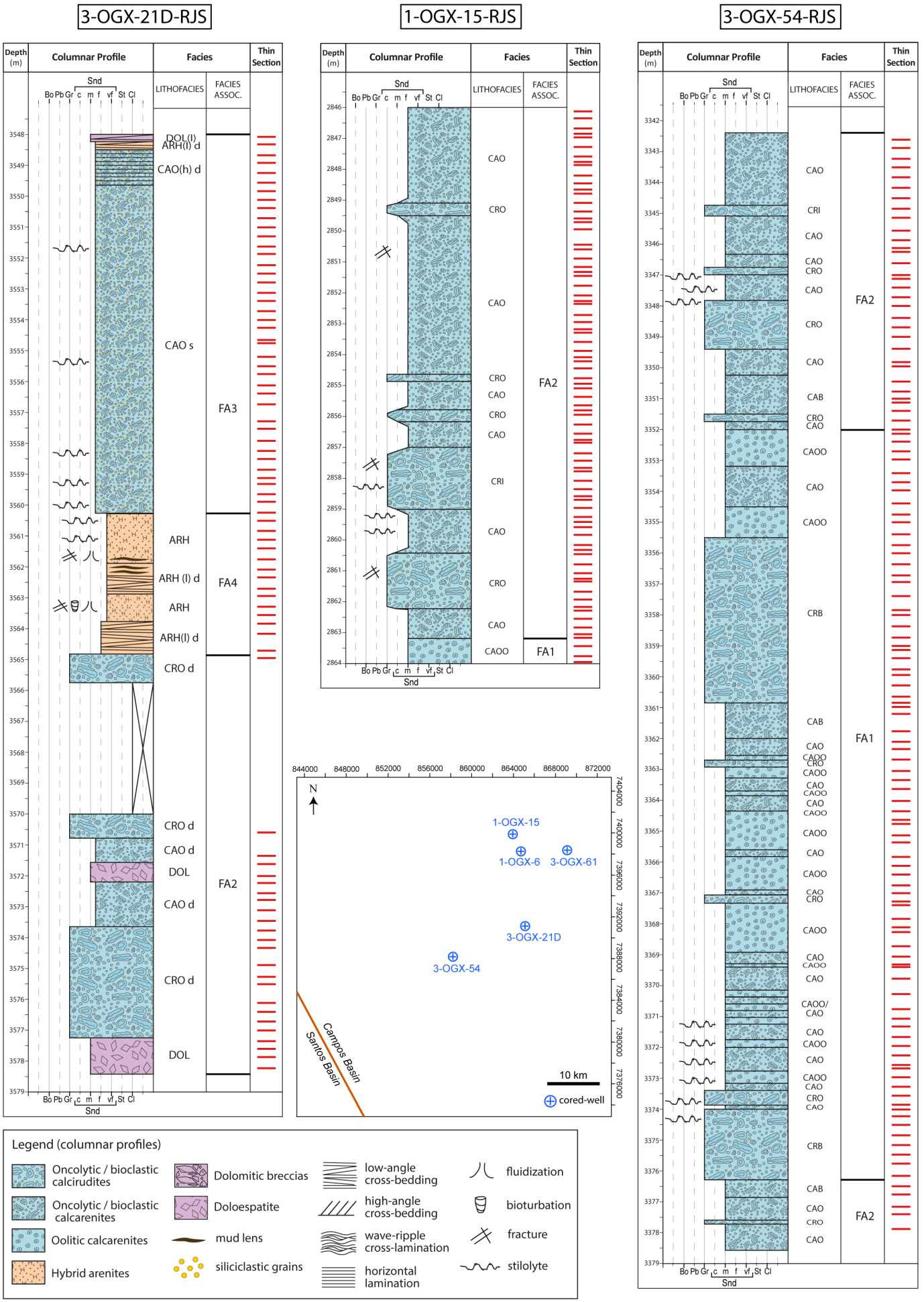

Figure 3 | Continued.

Facies	Description	Interpretation
CAOO	Oolitic calcarenites with variable proportions of oncolites, peloids and rare fragmented bioclasts from bivalves and echinoids (Figure 4A, B). May contain quartz, feldspars and micas. Massive, locally bioturbated and with stylolites and dissolution seams.	High-energy flows, massive strata resulting from post-depositional diagenesis, fluidization or bioturbation, obliterating the primary depositional structure.
CAO	Oncolytic / peloidal calcarenites, with variable proportions of oolites and fragmented bioclasts from bivalves, echinoids and gastropods. May contain quartz, feldspars and micas (Figure 4C). Massive, locally fractured, stylolitized and with dissolution seams. Bioturbation and dolomitization may occur.	Moderate-energy flows, massive strata resulting from post-depositional diagenesis or fluidization or bioturbation, obliterating the primary depositional structure.
CRO	Oncolytic calcirudites with variable proportions of intraclasts, peloids and fragmented bioclasts (echinoids, bivalves and gastropods) (Figure 4E). May contain quartz, feldspars and micas. Massive, locally fractured, stylolitized and with dissolution seams. Bioturbation and dolomitization may occur.	
CAO(x)	Oncolytic calcarenites, with variable proportions of peloids, oolites and fragmented bioclasts from bivalves, echinoids and gastropods. May contain quartz grains, feldspars and micas. High-angle cross-bedding; locally fluidized (Figure 4F).	Migration of subaqueous, sinuous-crested dunes under unidirectional to combined flow regime.
CRO(x)	Oncolytic calcirudite with variable proportions of intraclasts, peloids and fragmented bioclasts (echinoids, bivalves and gastropods), and with quartz, feldspars and micas. High-angle cross-bedding, fluidized (Figure 4D).	
CAO(l)	Oncolytic calcarenites, with variable proportions of peloids, oolites and fragmented bioclasts from bivalves, echinoids and gastropods. May contain quartz, feldspars and micas. Low-angle cross-bedding.	Migration of attenuated bedforms under the influence of critical unidirectional currents associated with oscillatory flows (combined flow regime).
CAOO(l)	Oolitic calcarenites with variable proportions of oncolites, peloids and rare fragmented bioclasts from bivalves and echinoids. May contain quartz grains, feldspars and micas. Low-angle cross-bedding, locally stylolitized and with dissolution seams.	
CAO(h)	Oncolitic calcarenite with peloids and rare fragmented bioclasts from bivalves, echinoids and gastropods, and with grains of quartz, feldspars and micas. Dolomitized, horizontal lamination.	Bedforms originated under low-energy flow regime.
CAB	Bioclastic calcarenites (fragmented, mainly bivalves, also echinoids, gastropods and, less commonly, crustaceans), with smaller proportions of oncolites, oolites and peloids.	High- to moderate-energy flows, massive resulting from post-depositional diagenesis or fluidization or bioturbation, obliterating the primary depositional structure.
CRB	Bioclastic calcirudites (fragmented, mainly bivalves, also echinoids, gastropods and, less commonly, ostracods, crustaceans, annelids and benthic foraminifera), with smaller proportions of oncolites, oolites and peloids. Locally stylolitized.	
ARH	Hybrid arenites composed of siliciclastic grains (quartz, feldspars and micas) and carbonate particles (oolites, oncolites, fragmented bioclasts and peloids). Rare mud lenses. Massive, locally dolomitized bioturbated, fluidized and fractured. Stylolites may occur.	Deposition from subaqueous hyper-concentrated gravity flows or, most likely, resulting from post-depositional diagenesis, bioturbations or fluidization, obliterating the primary depositional structure.
ARH(l)	Hybrid arenites composed of siliciclastic grains (quartz, feldspars and micas) and carbonate particles (oolites, oncolites, fragmented bioclasts and peloids). Rare mud lenses. Low-angle cross-bedding, often dolomitized (Figure 4G).	Migration of attenuated bedforms under the influence of critical unidirectional currents associated with oscillatory flows (combined flow regime).
ARH(x)	Hybrid arenites composed of siliciclastic grains (quartz, feldspars, micas) and carbonate particles (oolites, oncolites, fragmented bioclasts and peloids), with high-angle cross-bedding (Figure 4H). Often dolomitized.	Migration of sinuous-crested subaqueous bedforms under unidirectional to combined flow regime.
ARH(w)	Dolomitized hybrid arenites composed of siliciclastic grains (quartz, feldspars and micas) and carbonate particles (oolites, oncolites, fragmented bioclasts and peloids). Wave-ripple cross-lamination, locally bioturbated (Figure 4I).	Migration of ripples under oscillatory flow regime.

Table 1 | Lithofacies that compose the Quissamã Fm. with their description and interpretation.

ARH(w) (Table 1). The allochemical grains are either dissolved or completely replaced by blocky dolomite. Most of the siliciclastic constituents are partially replaced by dolomite. The remaining single-crystalline quartz grains and feldspars are predominantly angular to subangular (Figure 5A, B). These arenites are commonly fluidized and bioturbated, and rarely laminated, stylolitized or fractured (Figure 5C, D). Siliciclastic grain size varies from silt to coarse sand, with fine sand prevailing. The siliciclastic grains are, in order of abundance: monocrystalline quartz, K-feldspars (microcline and orthoclase), micas (muscovite and biotite), plagioclase, and heavy minerals (zircon, garnet, amphibole, tourmaline and titanite). Non-carbonate intrabasin constituents, including glauconite peloids, carbonaceous fragments, and muddy intraclasts, occur as traces (Table 3).

	Post-depositional facies
DOL	Dolosparite. Crystalline rocks with pervasive replacement of carbonate constituents by block dolomite. Massive, may exhibit wave-ripple cross-lamination and high- or low-angle cross-bedding.
BrD	Dolomitic breccias, fractured and stylolitized; carbonate constituents replaced by block dolomite. Rare quartz and feldspars. Locally fluidized.

Table 2 | Post-depositional facies of the Quissamã Fm.

4.1.2. Petrographic characterization of the (non-dolomitized) hybrid arenites

The hybrid arenite lithofacies ARH, ARH(x) and ARH(l) (Table 1) occur interbedded with moderate- to high-energy limestones (Figure 3). They are composed of siliciclastic and carbonate grains (Figure 6A; Table 4). These arenites are predominantly massive, fluidized, bioturbated, and rarely stylolitized or fractured (Figure 6B). The siliciclastic grains are predominantly monocrystalline quartz, K-feldspars (microcline and orthoclase), muscovite and

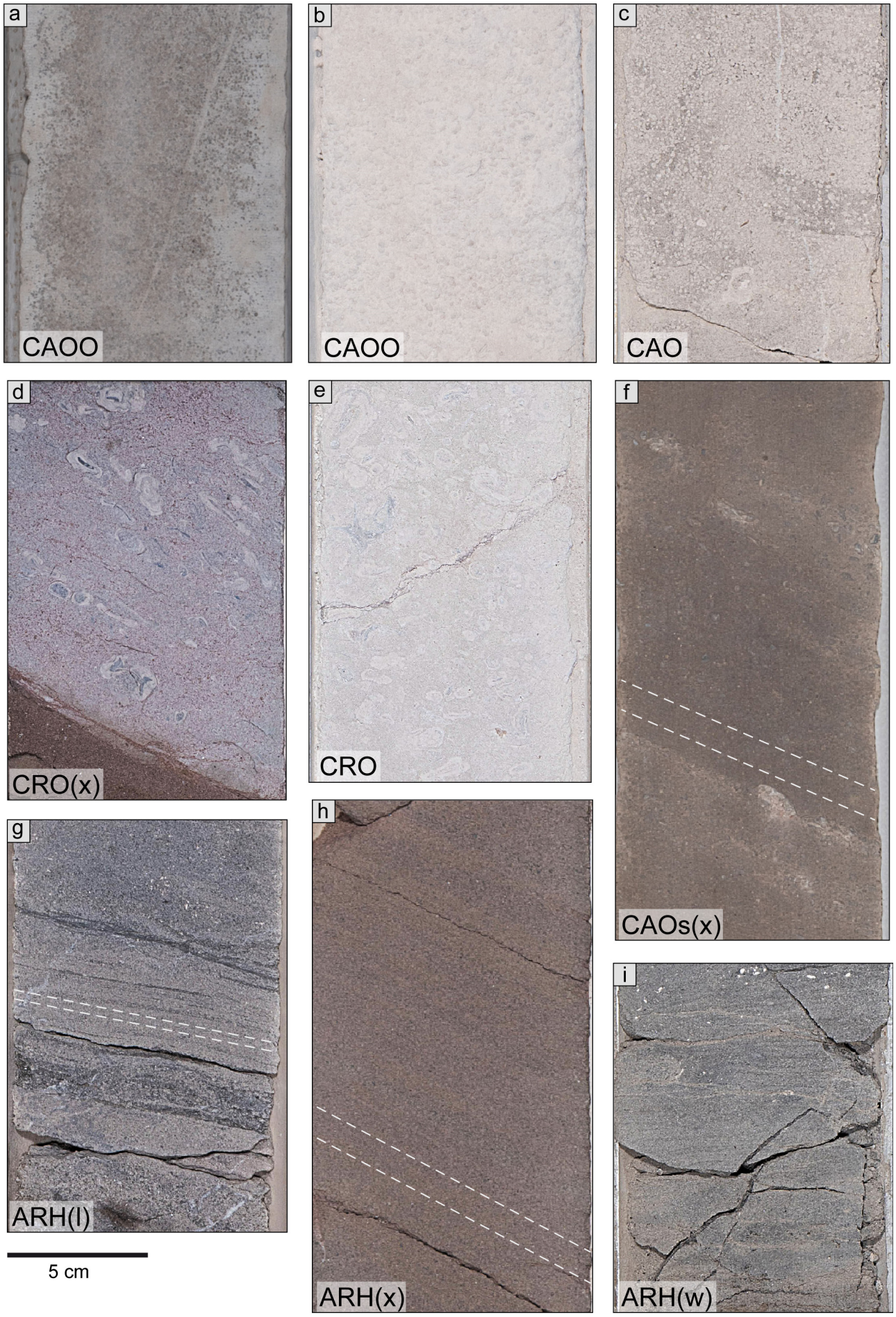

Figure 4 | Photos of the cored wells showing eight of the interpreted lithofacies: (A) and (B) oolitic calcarenites; (C) oncolytic calcarenite; (D) oncolytic calcirudite with high-angle cross-bedding marked by the orientation of the bioclasts; (E) oncolytic calcirudite; (F) oncolytic calcarenite with high-angle cross-bedding; (G) hybrid arenite with low-angle cross-bedding; (H) hybrid arenite with high-angle cross-bedding; (I) hybrid arenite with wave-ripple cross-lamination. Dashed white lines in (F), (G), and (H) indicate the angle and direction of cross-bedding.

Primary constituents	Average (%)	Maximum (%)
Monocrystalline quartz	9.6	17.7
K-feldspars	6.0	13.0
Plagioclase	<1	1.7
Micas	2.1	6.7
Heavy minerals	<1	0.7
Carbonaceous fragments	<1	0.7
Carbonate peloids	<1	0.3
Glauconite peloids	<1	0.7

Table 3 | Main primary constituents in the dolomitized hybrid arenites.

biotite. Plagioclase grains are rare (Figure 6C), and heavy minerals such as zircon, tourmaline, garnet, rutile and opaques are very rare, as are plutonic rock fragments and non-carbonate intrabasin constituents such as glauconite peloids, carbonaceous fragments and fish bones (Table 4). Most of the orthoclase grains have either been partially dissolved or replaced by kaolinite or calcite. Biotite grains are commonly replaced by pyrite. Siliciclastic grains are predominantly subangular, but angular grains are also common (Figure 6D). Siliciclastic grains vary in size from very fine to medium sand, with fine sand predominating. The range of carbonate grains range in size from coarse silt to granule. The hybrid arenites are moderately- to poorly-sorted; the poor sorting is due to allochemical particles (large bivalve bioclasts, carbonate sand intraclasts or microbials) (Figure 6E). Packing is predominantly tight and rarely normal, with predominantly straight intergranular contacts, followed by concave-convex and sutured (Figure 6F). The grain orientation is chaotic in most samples, due to fluidization or bioturbation processes; preserved laminations are rare. The most common allochemical constituents are, in order of abundance: peloids, oncolites, bioclasts, oolites, carbonate sand intraclasts and microbials (Table 4). Some oolites and oncolites have a core composed of quartz grains and feldspars, and rarely bioclasts. Many feldspars in oolite cores are partially dissolved or replaced by kaolinite, or with overgrowths of K-feldspar. Peloids and oolites range in size from very fine to medium sand, though are predominantly fine sand sized. The oncolites range in size from medium to very

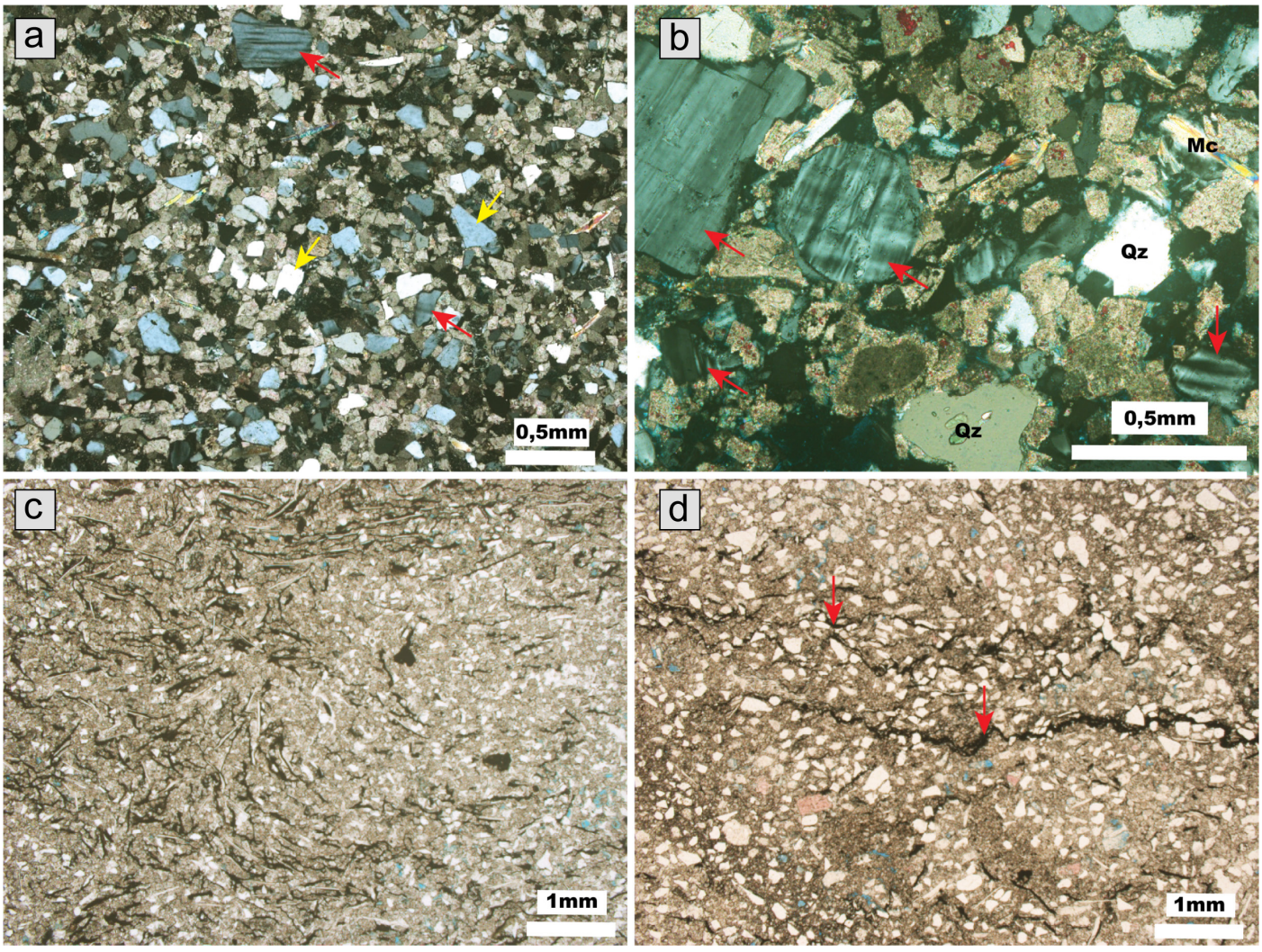

Figure 5 | Petrographic features of the dolomitized hybrid arenites. (A) Fine-grained, dolomitized hybrid arenite with angular and subangular grains of monocrystalline quartz and microcline. Crossed polarizers (XP); red arrows indicate K-feldspars, and yellow arrows indicate quartz. (B) Dolomitized hybrid arenite rich in microcline grains (XP); red arrows indicate K-feldspars (microcline); abbreviations: Qz (quartz) and Mc (muscovite). (C) Very-fine grained, bioturbated dolomitized hybrid arenite. Uncrossed polarizers (//P). (D) Fine-grained, stylolitized dolomitized hybrid arenite (//P); red arrows indicate stylolites.

Primary constituents	Average (%)	Maximun (%)
Monocrystalline quartz	15.3	21.3
K-feldspars	11.3	14.7
Plagioclase	1.3	3.0
Micas	2.3	5.7
Heavy minerals	<1	1.0
Carbonaceous fragments	<1	3.3
Microbial carbonate intraclasts	<1	5.3
Carbonate sand intraclasts	1.7	15.0
Carbonate peloids	21.6	53.3
Glauconite peloids	<1	1.0
Ooids	2.7	4.3
Oncoids	9.0	26.0
Carbonate bioclasts	4.7	6.0

Table 4 | Main primary constituents in the hybrid arenites.

coarse sand, and are predominantly coarse sand sized, while intraclasts range from coarse sand to granule size. Some oolites and oncolites show margin abrasion from reworking. Bioclasts are, in order of abundance: bivalves, echinoids, benthic foraminifera, ostracods, gastropods, red algae and planktonic foraminifera. All allochemicals are intensely micritized.

4.1.3. Petrographic characterization of carbonates

The identified carbonate lithological types in the Albian Campos Basin were grouped into the lithofacies CAO, CRO, CAOO, CAO(x), CRO(x), CAO(l), CAOO(l), CAO(h), CAB and CRB (Table 1).

Primary composition: simple and agglomerate oncolites, peloids, simple and polycompound oolites, microbial intraclasts and carbonate sand, with a commonly subordinate volume of bioclasts of bivalves, echinoids, red algae, benthic and planktonic foraminifera, gastropods, bryozoans, annelids, calcispheres, and ostracods, as well as siliciclastic grains of quartz, feldspars, micas, rock fragments and heavy minerals. Siliciclastic grains are less common, and normally occur as the nucleus of oolites and oncolites. Other primary constituents present in reduced volume are glauconite peloids, fish bioclasts, phosphatic peloids and carbonaceous fragments.

Oolitic calcarenites deposited under high-energy conditions are commonly massive or laminated (Figure 7A, B), and rarely stratified, fractured or stylolitized. Grain size varies from fine to coarse sand, with a mode of medium sand, well- to moderately-sorted. Rare poorly sorted samples are related to remobilized deposits (Figure 7C). Carbonate bioclasts are very rare in oolitic calcarenites, as are polycomposite oolites. Oncolithic/bioclastic calcarenites and moderate-energy oncolitic/intraclastic/bioclastic calcirudites range from poorly- to very poorly-sorted, with grain sizes ranging from silt to pebble, with a mode of coarse sand. They are commonly massive, stylolitized, fractured and rarely fluidized (Figures 7D and 8A, B). Oncolithic-peloidal calcarenites range from well- to moderately-sorted, with a mode of fine sand (Figure 8C). Low-energy deposits are represented by calcisiltites and calcilutites, commonly massive and rarely laminated, bioturbated or fluidized (Figure 8D).

4.2. Facies associations

The 14 described lithofacies in the five cored wells were grouped into four facies associations: FA1, carbonate shoal - shallower portion, FA2, carbonate shoal - deeper portion, FA3, hybrid shoal and FA4, coastal environment. The description and interpretation of all facies associations are summarized in Table 5.

FA1: Carbonate shoal - shallower portion

Facies Association 1 (FA1) is present in three of the described cored wells: 3-OGX-61, 1-OGX-15 and 3-OGX-54, and has a maximum thickness of 24.3 m (Figure 3). FA1 predominantly comprises oolitic and oncolytic calcarenites (CAOO and CAO), accounting for 70% of the lithofacies (Figure 9). Oncolytic and bioclastic calcirudites (CRO and CRB), are common (summing 28%), and bioclastic calcarenites (CAB) are rare (2%). The described lithofacies are massive. Bioturbation occurs on well 3-OGX-61, where stylolites and dissolution seams are common.

Environmental Interpretation: oolites form in high-energy environments, in agitated waters where they are frequently moved as dunes or ripples by currents and/or wave action (Tucker, 2001). The primary depositional structures are likely obliterated due to either post-depositional diagenesis, fluidization or bioturbation (Miall, 1978). The significant presence of oolitic calcarenites in a sequence of purely carbonate rocks indicate this FA is the shallow portion of a carbonate shoal (Wilson, 1975; Veeken & Moerkerken, 2013), located distal from a siliciclastic input region.

FA2: Carbonate shoal - deeper portion

Facies association 2 (FA2) is present in all five described cored wells, and has a maximum thickness of 17.6 m (Figure 3). It is mainly composed of oncolitic calcarenites and calcirudites (CAO and CRO), summing 96% of the FA2 lithofacies (Figure 9). Bioclastic calcarenite is also present (4%), and there are doloesparites in well 3-OGX-21D. The described lithofacies are massive. Bioturbation and fractures occur locally; stylolites and dissolution seams are common.

Environmental Interpretation: the vertical succession of oncolitic calcarenites and calcirudites indicate the hydrodynamic energy was high enough to keep moving the bioclasts, oncoliths and peloids (Dahanayake, 1978). However, water energy is not enough to trigger the formation of

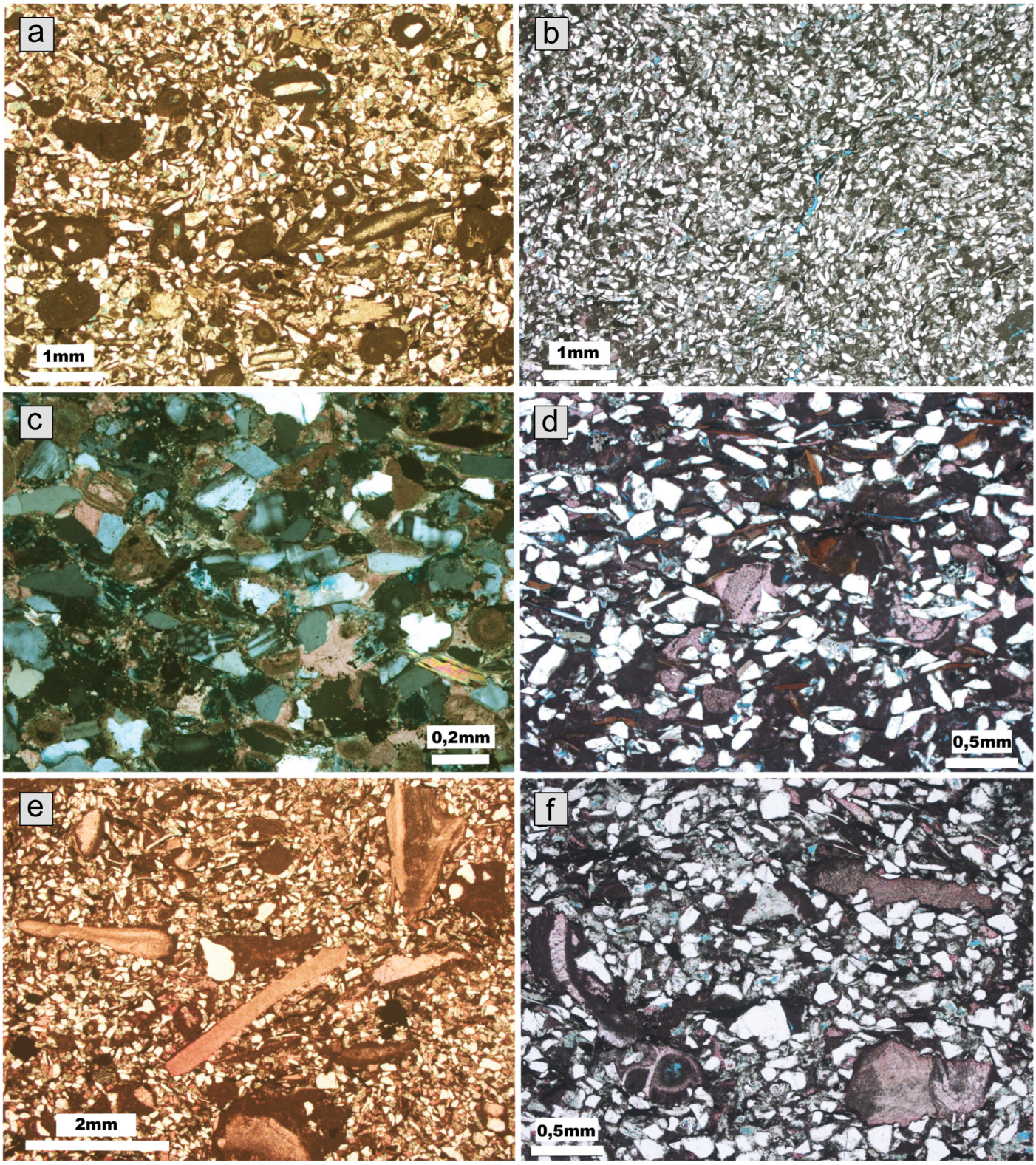

Figure 6 | Petrographic features of the hybrid arenites. (A) Fine-grained hybrid arenite constituted by siliciclastic grains and carbonate ooliths, oncoliths and bivalve bioclasts. Uncrossed polarizers (//P). (B) Very fine-grained, fluidized hybrid arenite (//P). (C) Hybrid arenite rich in K-feldspar grains (microcline). Crossed polarizers (XP). (D) Angular to subangular siliciclastic grains in hybrid arenite rich in peloids (//P). (E) Poorly-sorted hybrid arenite with large bivalve bioclasts and oncoliths (//P). (F) Compacted hybrid arenite with penetration of the bioclasts by the siliciclastic grains; framework closed by compaction (//P).

ooids (Simone, 1980). Therefore, we interpret that FA2 formed in a moderate-energy subaqueous environment, with less intense or frequent water agitation, consistent with protected areas between oolitic shoal crests (Okubo et al., 2015). The lithofacies are massive likely because post-depositional diagenesis, fluidization or bioturbation obliterated the primary depositional structure.

FA3: Hybrid (carbonate-siliciclastic) shoal

Facies association 3 (FA3) is only present in the wells 1-OGX-6 and 3-OGX-21D, with thickness of up to 18.3 m (Figure 3). FA3 predominantly comprises oncolytic and oolitic calcarenites and calcirudites with 10 to 30% of siliciclastic constituents, totaling 91% of the lithofacies (Figure 9). Hybrid arenites and oncolytic calcarenites are less

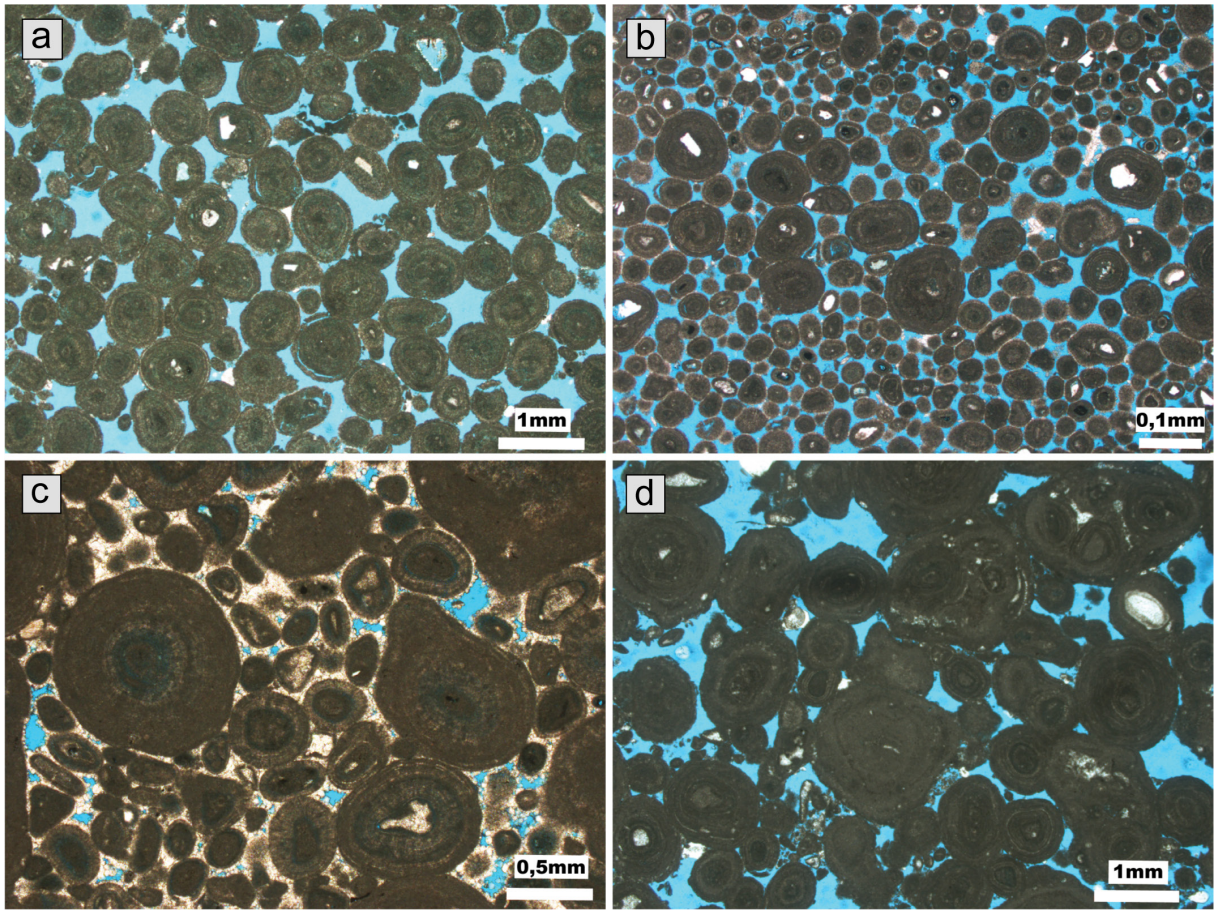

Figure 7 | Petrographic features of the carbonates. (A) Medium-grained oolitic calcarenite, massive and well-sorted. Uncrossed polarizers (//P). (B) Laminated oolitic calcarenite with primary interparticle porosity (//P). (C) Poorly-sorted, redeposited oolitic calcarenite, cemented by calcite rims (//P). (D) Poorly-sorted oncolitic calcarenite with interparticle porosity (//P).

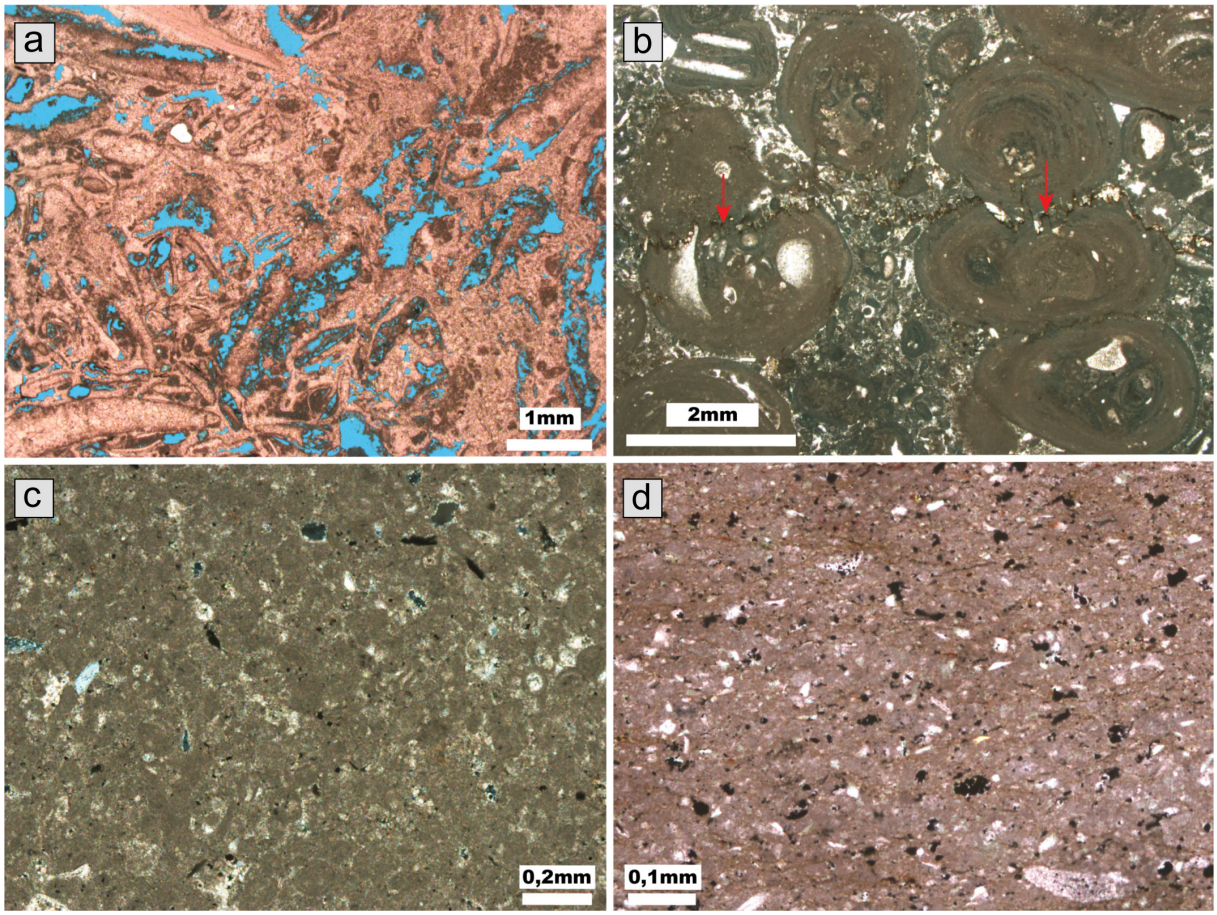

Figure 8 | Petrographic features of the carbonates. (A) Bioclastic calcirudite cemented by calcite (stained pink) with moldic and vuggy porosity. Uncrossed polarizers (//P). (B) Compacted oncolitic calcirudite with stylolites (indicated with red arrows) (//P). (C) Well-sorted, compacted peloidal calcarenite (//P). (D) Peloidal calcisiltite with microcrystalline pyrite replacing undifferentiated grains (//P).

Facies associations	Description	Interpretation
FA 1	Calcarenites (and secondary calcirudites) with oolites and oncolites, and less commonly peloids and bioclasts (bivalves and echinoids); massive, locally bioturbated, stylolitized and dissolution seams.	Carbonate shoal, shallower portion, with higher energy.
FA 2	Calcarenites and calcirudites with oncolites, and variable amounts of peloids, oolites, bioclasts (bivalves, echinoids, gastropods) and intraclasts; massive, locally fractured and bioturbated. Rare occurrence of dolosparites. Stylolites and dissolution seams are common.	Carbonate shoal, deeper portion, with lower energy.
FA 3	Hybrid arenites with quartz, feldspar, micas, rare mud lenses and carbonate components (oncolites, oolites, peloids and bioclasts), and calcarenites and calcirudites with variable proportions of oncolites, oolites, bioclasts, peloids and intraclasts, and more than 10% siliciclastic components (quartz, feldspar, and micas). Massive or with high- or low-angle cross-bedding, and one occurrence of horizontal lamination. Locally stylolitized, fluidized, fractured and bioturbated.	Hybrid shoal (with significant siliciclastic input), deeper portion, lower energy.
FA 4	Hybrid arenites, dolosparites and carbonate breccias, with grains of quartz, feldspar, micas and carbonate components (oolites, oncolites, peloids and bioclasts). Massive or with high- or low-angle cross-bedding, and wave-ripple cross-lamination. Locally stylolitized, fluidized, fractured and bioturbated.	Coastal environment; presence of oscillatory and current flows induced by waves.

Table 5 | Summary of the interpreted facies association with their description and interpretation.

frequent. The described lithofacies are dominantly massive, but high- and low-angle cross-bedding are common. Fluidization, stylolites, bioturbation and fractures occur locally.

Environmental Interpretation: the presence of low- and high-angle cross-bedding indicate bedform migration under critical- to supercritical-unidirectional currents associated with combined flow regime (Dumas et al., 2005; Ferronatto et al., 2021). The dominance of carbonate facies with a significant percentage of siliciclastic particles, and deposition under combined flow conditions, indicate a hybrid shoal environment, located close to a region of siliciclastic input (Chiarella et al., 2017).

FA4: Coastal environment

Facies association 4 (FA4) is found in wells 3-OGX-61, 3-OGX-21 and 1-OGX-6, measuring up to 31 m of thickness (Figure 3). FA4 dominantly consists of hybrid arenites (ARH), summing 93% of the lithofacies; siliciclastic oncolytic calcarenites compose the remaining 7% (Figure 9). Post-depositional facies, dolosparite (DOL) and dolomic breccies (BrD), are common in well 1-OGX-6. The described lithofacies are either massive, with high- or low-angle cross-bedding, or with wave-ripple cross-lamination. Fluidization, stylolite, bioturbation and fractures occur locally.

Environmental Interpretation: the occurrence of both high- and low-angle cross-bedding and wave-ripple cross-lamination indicate a combined oscillatory and current flow regime induced by waves (Dumas et al., 2005; Ferronatto et al., 2021). This FA is dominated by hybrid arenites, which, coupled with the set of sedimentary structures observed, indicate a more proximal (i.e., coastal) environment.

4.3. Depositional model and facies succession

Through the integration of rock and petrophysical data, we subdivided the Albian interval of the Campos Basin (the Macaé Group; Figure 1) into three chronostratigraphic units: MAC1, MAC2 and MAC3, from base to top, separated by flooding surfaces (sensu Catuneanu et al., 2011) evidenced by positive peaks in the gamma rays curves (Figures 10 and 11). The basal units, MAC1 and MAC2, correspond to the lower Albian interval (Quissamã Fm.), and the top unit, MAC3, to the upper Albian (Outeiro Fm, Figure 1). It is observed that the carbonates and hybrid sandstones interpreted in the MAC1 and MAC2 units give way to intercalations of shales and calcilutites in MAC3 (Figure 10).

Facies analysis and the spatio-temporal framework of the interpreted units indicate that the depositional model of the SW Campos Basin is a carbonate ramp (sensu Burchette & Wright, 1992) or a rimmed carbonate platform (sensu Bosence, 2005), with significant siliciclastic input locally (Figure 12). The ramp is divided into four parts, which are (from proximal to distal): coastal environment, internal ramp (backshoal), intermediate ramp (carbonate and hybrid shoals), and external ramp.
The isolith maps of the Albian interval of the SW Campos Basin indicate distinct areas of greater and lesser concentrations of carbonate and hybrid facies. It is observed that carbonate facies have a greater concentration in four elongate areas with NE-SW orientation (Figure 13A – numbers 1 to 4). The highest concentration of hybrid beds occurs towards the coast (NW) and between intermediate regions with greater concentration of carbonates, and overall decrease towards the basin (SE) (Figure 13B).

5. Discussion

5.1. Carbonate–siliciclastic mixing

We describe 14 lithofacies, 10 of which are carbonate and 4 are hybrid arenites (Table 1). The hybrid arenites are composed of carbonate particles and at least 30% of siliciclastic constituents (Zuffa, 1980). In terms of composition, the siliciclastic grains are, in order of abundance: monocrystalline quartz, K-feldspars (microcline and orthoclase) and micas (muscovite and biotite); plagioclase and heavy minerals are rare (Tables 3 and 4). Carbonate facies are dominantly composed of carbonate particles, mainly non-skeletal constituents, including oncolites, peloids, oolites and microbial intraclasts; bioclasts occur subordinately (of bivalves, echinoids, red algae, benthic and planktonic foraminifera, gastropods, bryozoans, annelids,

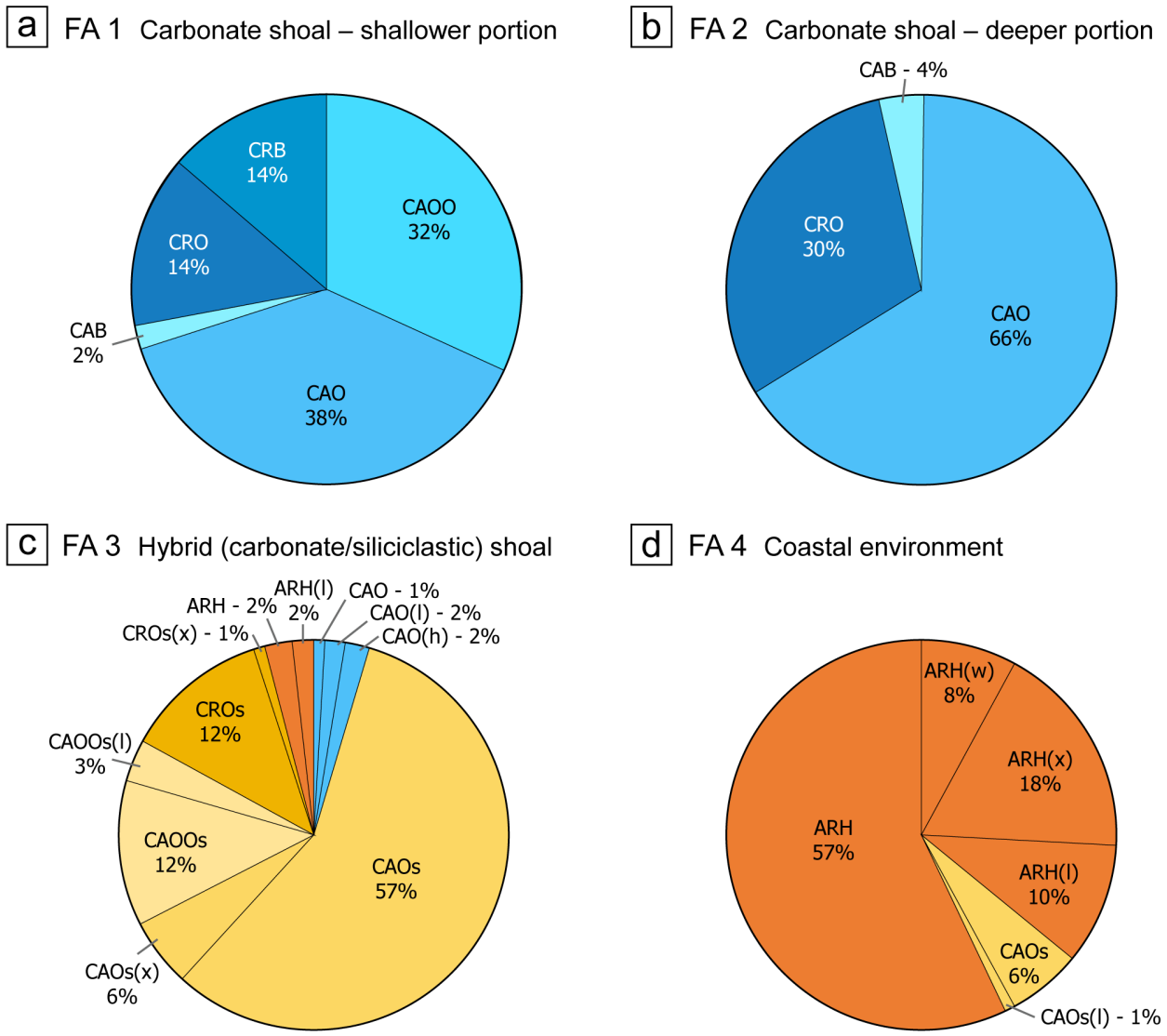

Figure 9 | Pie charts showing the percentage of lithofacies per facies associations. See Table 1 for description of lithofacies.

calcispheres and ostracods) (Figure 7). Siliciclastic grains are present in varying proportions (up to 30% of the total constituents), and commonly occur only as the nucleus of oolites and oncolites.

Mixing of siliciclastic and carbonate constituents can occur in different depositional arrangements. In our study we recognize mainly the compositional mixing at bed and lithofacies scale (millimetre to meter) (sensu Chiarella et al., 2017). However, strata mixing at lithofacies and stratigraphic scale (meters to tens of meters) is also present considering that hybrid arenite facies commonly occur interbedded with carbonate facies (Figure 3), and the proportion of carbonate and siliciclastic components vary in space (Figure 13).

Compositional-mixing occurs in situ where there is contemporaneous availability in space and time of siliciclastic and carbonate sources (Chiarella et al., 2017). It is directly influenced by the depositional processes active during sedimentation. In shallow marine settings, these processes are related to the interplay between waves, currents and tides transporting and depositing the sediments (Schwarz et al., 2018). Waves and associated currents are the primary drivers of sediment transport, mixing, and deposition, generating layers with varying proportions of carbonate and siliciclastic particles.

Stratal-mixing occurs along boundaries between contrasting, siliciclastic- versus carbonate-dominated environments, such as flanks of carbonate shoal complexes that shelter siliciclastic lagoons, or on mid-shelf environments where carbonate and siliciclastic layers interfinger (Chiarella et al., 2017; McNeill et al., 2012). This mixing can be the result of either autocyclic or allocyclic factors, or the contemporaneous action of both. Autocyclicity develops due to unforced internal dynamics of carbonate and siliciclastic sedimentation in response to subsidence (Thrana & Talbot, 2006), which is complex and strongly influenced by salt tectonics during the Albian in the Campos Basin. Allocyclic factors influence the relative importance of siliciclastic sediment supply versus carbonate production, and affect sediment dispersal (Chiarella & Longhitano, 2012). These include: high-frequency sea-level variations, climate changes from arid to humid conditions, or a tectonic control on the sediment supply from the continent (Chiarella et al., 2017; Tanavsuu-Milkeviciene et al., 2009).

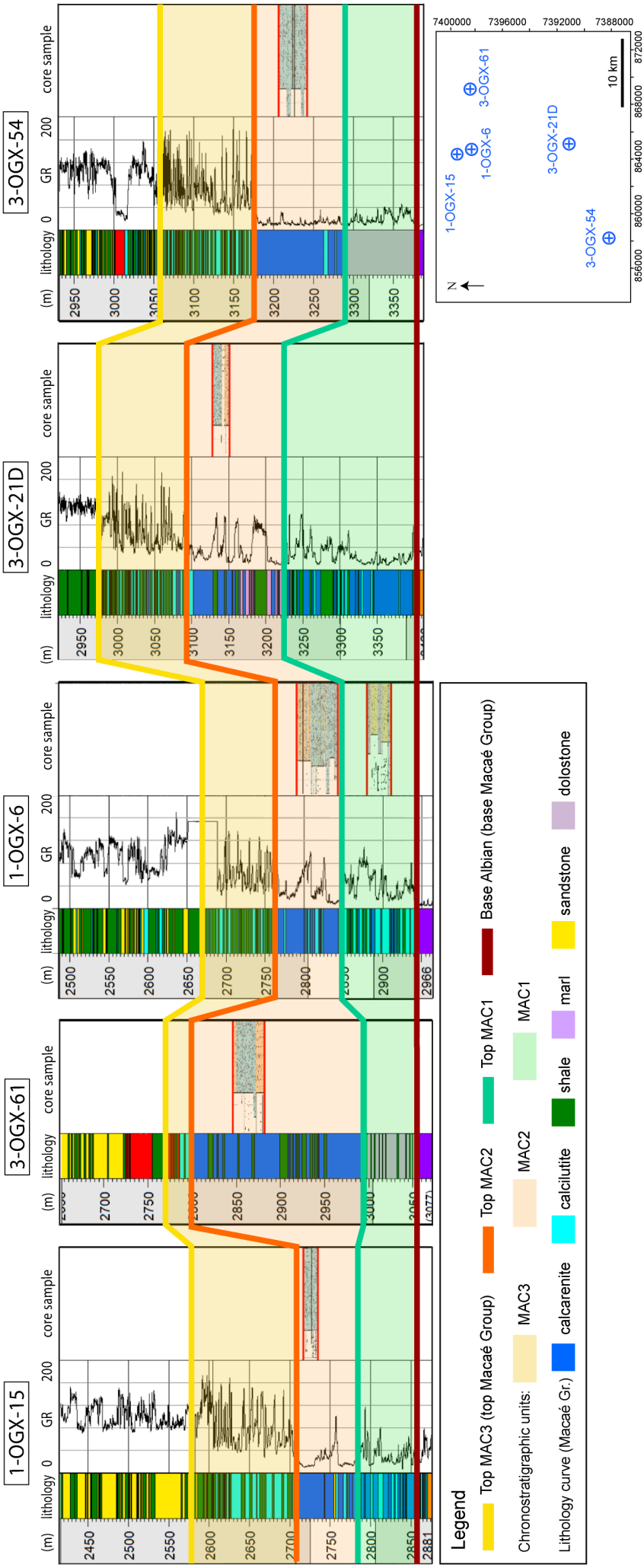

Figure 10 | Correlation section between wells with described core samples (see Figure 3), showing interpreted chronostratigraphic units (MAC1, MAC2 and MAC3) and bounding surfaces. The map in the lower right shows the location of the wells.

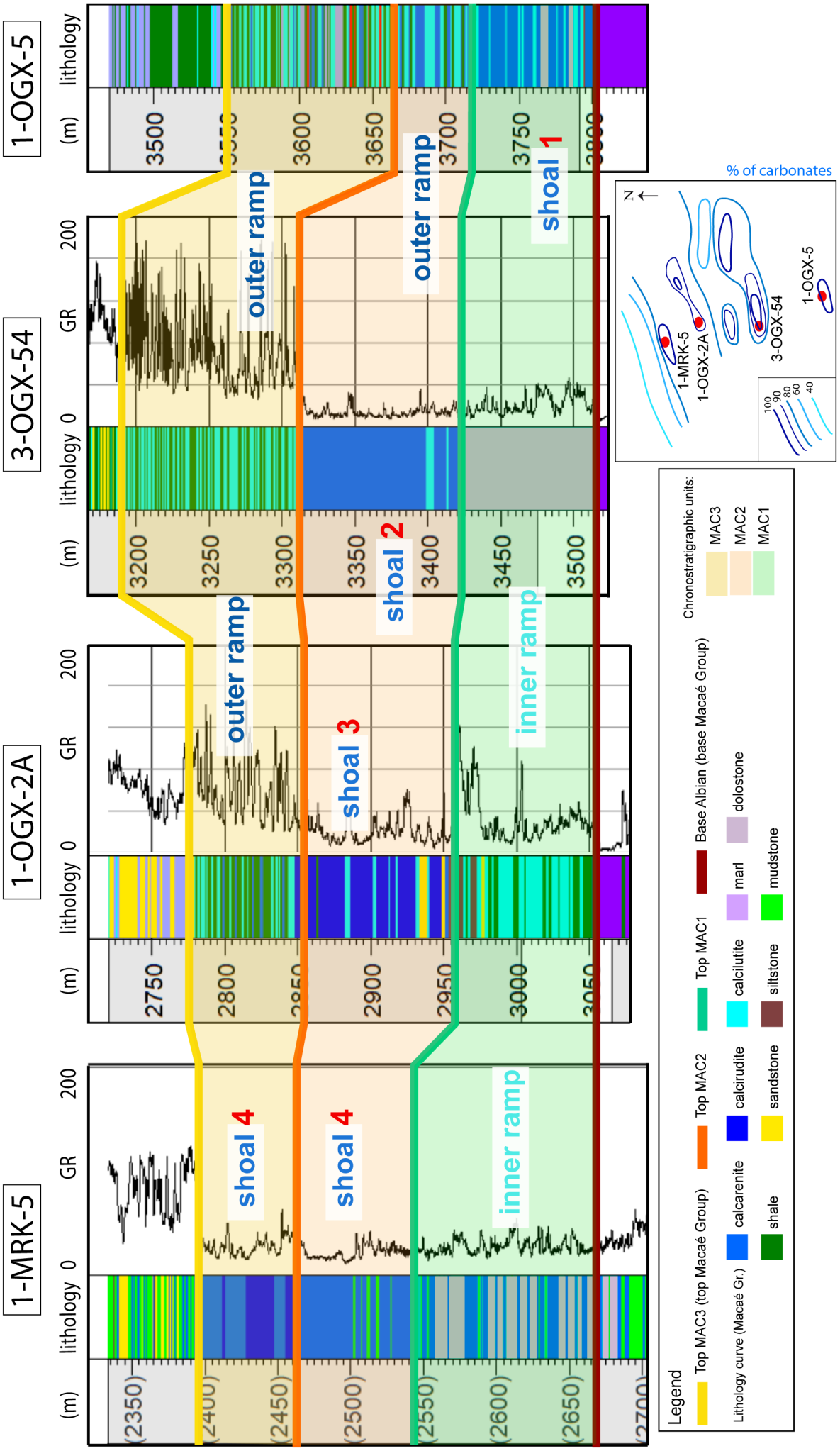

Figure 11 | Dip-oriented (NW-SE) correlation section across the four interpreted carbonate shoals (areas with highest percentage of carbonate facies), with the interpreted facies associations, chronostratigraphic units (MAC1, MAC2 and MAC3) and bounding surfaces. The numbered shoals correspond to the numbered areas in Figure 13. The map in the lower right shows the location of the wells.

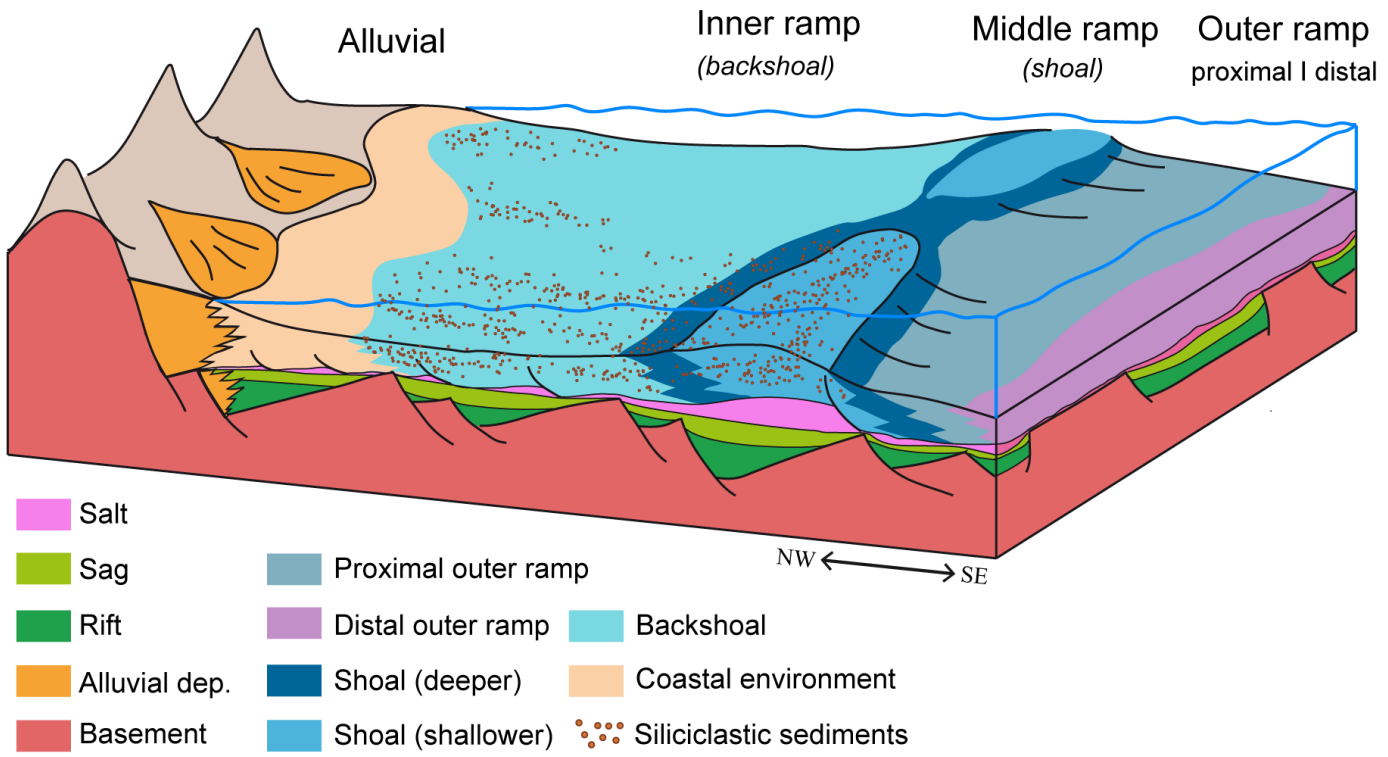

Figure 12 | Depositional model of the Albian interval of the SW Campos Basin - carbonate ramp (sensu Burchette & Wright, 1992).

Paleoecological studies of the Albian in the Campos Basin suggest that sediments were deposited under warm and arid climatic conditions (Dias-Brito & Azevedo, 1986; Koutsoukos, 1984; Rodrigues & Takaki, 1987; Armelenti et al., 2021). Structural highs limited the free circulation of oceanic waters from the narrow proto-Atlantic Sea during this time, promoting restricted, shallow water (less than 30 m), hypersaline environments (Azevedo, 2004). These environmental conditions allowed the development of a relatively scarce and low-diversity biota which includes episodic occurrences of opportunistic species (Guardado et al., 1989). Arid continental conditions indicate that river discharge and siliciclastic sediment supply are associated with isolated entry points, leaving several kilometres of the remaining shoreline without direct siliciclastic sediment input (Schwarz et al., 2018). Lithofacies in the Quissamã Formation have been interpreted as shallowing-upward cycles bounded by episodic flooding surfaces (Guardado et al., 1989; Rebelo et al., 2021; Favoreto et al., 2015; Okubo et al., 2015), indicative of high-frequency cycles of rising sea level, which can alter the positioning of facies belts, modifying the distribution of carbonate and siliclastic sediments. Additionally, major seaward translation of the Aptian evaporites began in the Albian (Quirk et al., 2012), resulting in salt structures that modified the topography, controlling the sediment dispersal routes.

We conclude that carbonate-siliciclastic mixing in the Albian of the Campos Basin occurs in different scales (bed, lithofacies and stratigraphic scales), and is caused by a combination of different factors: (i) in situ mixing related to the interplay between waves and currents transporting and depositing the sediments, resulting in compositional-mixing; (ii) high-frequency cycles of base level rise, causing a retreat of the hybrid system towards the continent; and (iii) salt tectonics influencing sediment dispersal patterns and the development and geometry of shoals.

5.2. Stratigraphic succession of the Albian of SW Campos Basin

Our work supports the previously published depositional model of the Albian Campos Basin: a carbonate ramp (sensu Burchette & Wright, 1992) sloping toward the east and NE with elongate NE-trending shoals (Guardado et al., 1989). Based on rock and geophysical data, we subdivided the Albian interval of Campos Basin into three chronostratigraphic units separated by flooding surfaces (sensu Catuneanu et al., 2011): MAC1, MAC2 and MAC3, from base to top. The vertical stacking of the units shows continuous retrogradation during the Albian interval of deposition in the basin, indicating a gradual increase in relative sea level and accommodation space.

The isolith maps indicate four elongate, NE-trending areas of greater carbonate facies (Figure 13A – numbers 1 to 4) which we interpret as carbonate shoals (following Guardado et al., 1989). The distance between the wells prevents precise measurements, but the most well-defined shoal crests measure from 2.5 to 7 km long and 1 to 2.2 km wide. The maximum thickness of the shoal crest is 24.3 m (Figure 3). Previous work describes Albian shoals of 20 m of thickness, elongated up to 2.5 km long and 1 km wide (Bruhn et al., 2003). The lateral correlation section (dip direction) in Figure 11, made with four wells in areas with the highest concentration of carbonate facies, indicates that the four carbonate shoals did not coexist,

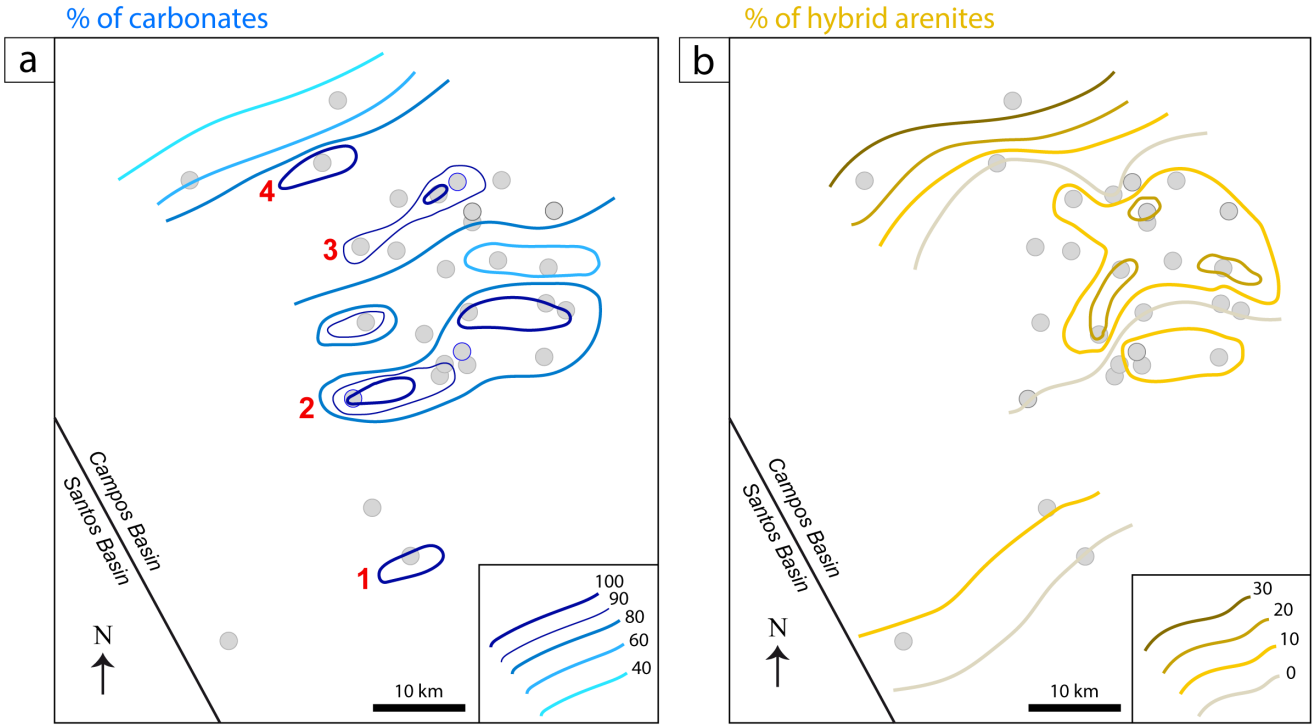

Figure 13 | Isolith maps showing the proportion of carbonate (A) and hybrid carbonate-siliciclastic (B) facies. The four numbered areas in (A) correspond to the shoals in Figure 11.

and are of different ages. The most distal carbonate shoal is older, forming part of the most basal unit, MAC1 (Figure 11 – number 1). Intermediate carbonate shoals are found in unit MAC2 (Figure 11 – numbers 2 and 3). The proximal shoal is the youngest, with deposition between the end of unit MAC2 and during unit MAC3 (Figure 11 – number 4). This demonstrates that the retrogradation of the Macaé Group (Albian) occurred in pulses, with high-frequency transgressive and relative sea level stabilization intervals, subordinate to a general transgressive trend.

Halokinetic movements and salt tectonics were in place during the deposition of the Albian succession (Quirk et al., 2012; Amarante et al., 2021). Previous works state that the position and geometry of shoals were controlled by the underlying evaporite configuration, i.e., shoals developed on salt pillows and/or rollers (Figueiredo & Mohriak, 1984; Guardado et al., 1989; Spadini et al., 1988). Our work shows that high-frequency sea level variations also influenced the position of the shoals, causing them to shift towards the shoreline over time.

The highest concentration of hybrid beds occurs on the flanks of carbonate shoals, and increases towards the coast (Figure 13B). These intershoal regions are the product of variations in depositional energy between the bank crests, and can be compared to deposits of sandy peloidal sheets of the inner platform defined by Spadini (1992). In our study, intershoal regions (i.e., flanks of shoals) can be hybrid or carbonate, indicating spatial and temporal variations in the siliciclastic input.

6. Conclusions

We integrate petrographic, sedimentological and geophysical data to characterize the depositional model, stratigraphic succession and sedimentation controls of the Albian interval of SW Campos Basin. The key conclusions of our study are:

- The Quissamã Formation (Albian) is composed of 14 lithofacies, 10 of which are limestones (with varying proportions of siliciclastic particles) and 4 are hybrid arenites. Carbonate particles are mainly non-skeletal constituents, including oncolites, peloids, oolites and microbial intraclasts; bioclasts occur subordinately. Siliciclastic grains are dominantly of monocrystalline quartz, K-feldspars (microcline and orthoclase) and micas (muscovite and biotite), and rarely plagioclase and heavy minerals.

- The identified lithofacies are grouped into four facies associations: carbonate shoal (shallower and deeper portions), hybrid carbonate-siliciclastic shoal and coastal environment. The shallower portions of carbonate shoal predominantly comprises massive oolitic and oncolytic calcarenites, and the deeper portions are mainly composed of massive oncolitic calcarenites and calcirudites. Hybrid carbonate-siliciclastic shoals predominantly present oncolitic and oolitic calcarenites and calcirudites with 10 to 30% of siliciclastic constituents, dominantly massive, or with high- and low-angle cross-bedding. The coastal environment consists mainly of massive hybrid arenites, however sedimentary structures (with high- and low-angle cross-bedding, and wave-ripple cross-lamination) are common.

- The Albian interval of the Campos Basin (Macaé Group) is divided into three chronostratigraphic units (MAC1 to MAC3 from base to top) separated by flooding surfaces. The stratigraphic succession of the units shows continuous retrogradation during the Albian interval of deposition in the basin.

- The depositional model of the SW Campos Basin is a carbonate ramp (sensu Burchette and Wright, 1992) or a rimmed carbonate platform (sensu Bosence, 2005), with significant siliciclastic input locally.

- Mixing of siliciclastic and carbonate constituents occurs as compositional mixing at bed scale, and strata mixing at lithofacies and stratigraphic scales (sensu Chiarella et al., 2017). Carbonate-siliciclastic mixture is caused by a combination of allocyclic and autocyclic factors, including the interplay between waves and currents, high-frequency cycles of base level rise, and salt tectonics.

- Isolith maps of siliciclastic and carbonate facies of Quissamã Formation indicate the existence of four NE-trending shoals, measuring 2.5 to 7 km long, 1 to 2.2 km wide, and up to 24.3 m thick.

- Dip-oriented correlation sections indicate that the shoals were non-contemporary. The most distal shoal is older, being part of MAC1; intermediate shoals were deposited during MAC2 and the proximal shoal is younger, with deposition between the end of unit MAC2 and during unit MAC3.

- The temporal and spatial distribution of the shoals define a retrograding backstepping pattern of the Albian in the Campos Basin.

Acknowledgements

The authors gratefully acknowledge Shell Brasil for the support to this study through the project: *Multidisciplinary Integrated Study of the Albian in the Santos, Campos and Espírito Santo Basins*, developed at COPPE/UFRJ and UFRGS. We thank the two anonymous reviewers for their constructive insights, and the executive editor Stéphane Bodin for his editorial handling. We also thank the strategic action of ANP (Brazil's National Oil, Natural Gas and Biofuels Agency) through the R&D levy regulation.

Author contribution

Francyne Bochi do Amarante - Writing – original draft; Conceptualization; Methodology; Investigation; Formal analysis. Claiton Marlon dos Santos Scherer - Writing – review and editing; Conceptualization; Methodology; Investigation; Formal analysis. Garibaldi Armelenti - Writing – original draft; Conceptualization; Methodology; Investigation. Luiz Fernando De Ros - Methodology; Investigation. Renata Alvarenga - Methodology; Investigation. Juliano Kuchle - Methodology; Investigation. João Claudio Conceição - Project administration; Funding acquisition; Final approval. José Luis Alves - Project administration; Funding acquisition; Supervision; Final approval. Luiz Landau - Project administration; Funding acquisition; Supervision; Final approval.

Data availability

The seismic and well data supporting this study were made available by ANP (Brazilian Agency of Petroleum, Natural Gas and Biofuels). The authors are not allowed to share the data, which were used under license for this study. For additional information, please contact help-desk@anp.gov.br.

Conflict of interest

The authors declare no conflict of interest.

References

Abelha, M., & Petersohn, E. (2018). The state of art of the Brazilian pre-salt exploration. AAPG Search and Discovery Article, #30586.

Amarante, F. B., Jackson, C. A.-L., Pichel, L. M., Scherer, C. M. S., & Kuchle, J. (2021). Pre-salt rift morphology controls salt tectonics in the Campos Basin, offshore SE Brazil. Basin Research, 33(5), 2837–2861. https://doi.org/10.1111/bre.12588

Amarante, F. B. D., Kuchle, J., Jackson, C. A., Scherer, C. M. D. S., & Pichel, L. M. (2023). The cryptic stratigraphic record of the syn- to post-rift transition in the offshore Campos Basin, SE Brazil. Basin Research, 36 (1). https://doi.org/10.1111/bre.12820

Amorosi, A., & Zuffa, G. G. (2011). Sand composition changes across key boundaries of siliciclastic and hybrid depositional sequences. Sedimentary Geology, 236, 153–163. https://doi.org/10.1016/j.sedgeo.2011.01.003

Armelenti, G., Goldberg, K., Alvarenga, R., Kuchle, J., Amarante, F. B., Scherer, C. S., Bastos, A. C., Conceição, J. C., Alves, J., & De Ros, L. (2021). Depositional and diagenetic impacts on the porosity of post-salt carbonate reservoirs of southern Campos Basin, southeastern Brazilian margin. Journal of South American Earth Sciences, 103566. https://doi.org/10.1016/j.jsames.2021.103566

Azevedo, R. L. M. (2004). Paleoceanografia e a evoluçao do Atlantico Sul no Albiano. Boletim de Geociências Petrobras, 12, 231–249.

Betzler, C., Braga, J. C., Jaramillo-Vogel, D., Römer, M., Hubscher, C., Schmiedl, G., & Lindhorst, S. (2011). Late Pleistocene and Holocene cool-water carbonates of the Western Mediterranean Sea. Sedimentology, 58, 643–669. https://doi.org/10.1111/j.1365-3091.2010.01177.x

Bosence, D. (2005). Carbonate shorelines and shelves. In R. C. Selley, I. R. Plimer, & L. R. M. Cocks (Eds.), Encyclopedia of geology (pp. 501–513). Elsevier. https://doi.org/10.1016/B0-12-369396-9/00178-7

Braga, J. C., de Neira, A. D., Lasseur, E., Mediato, J., Aguirre, J., Abad, M., Hernaiz-Huerta, P. P., Monthel, J., Perez-Valera, F., & Lopera, E. (2012). Pliocene-lower Pleistocene shallow-water mixed siliciclastics and carbonates (Yanigua and

Los Haitises formations) in eastern Hispaniola (Dominican Republic). Sedimentary Geology, 265–266, 182–194. https://doi.org/10.1016/j.sedgeo.2012.04.007

Bramkamp, R. A., & Powers, R. W. (1958). Classification of Arabian carbonate rocks. Bulletin of the Geological Society of America, 69, 1305–1317. https://doi.org/10.1130/0016-7606(1958)69[1305:COACR]2.0.CO;2

Bruhn, C. H. L., Gomes, J. A. T., Del Lucchese, C., Jr., & Johann, P. R. S. (2003). Campos Basin: Reservoir characterization and management - Historical overview and future challenges. In Offshore Technology Conference (OTC 15220). Houston, Texas, U.S.A. https://doi.org/10.4043/15220-ms

Burchette, T. P., & Wright, V. P. (1992). Carbonate ramp depositional systems. Sedimentary Geology, 79, 3–57. https://doi.org/10.1016/0037-0738(92)90003-A

Carozzi, A. V., & Falkenhein, F. U. H. (1985). Depositional and diagenetic evolution of Cretaceous oncolitic packstone reservoirs, Macaé Formation, Campos Basin, offshore Brazil. In P. O. Roehl & P. W. Choquette (Eds.), Carbonate petroleum reservoirs (pp. 317–343). Springer. https://doi.org/10.1007/978-1-4612-5040-1_30

Carozzi, A. V., Falkenhein, F. U. H., & Franke, M. R. (1983). Depositional environment, diagenesis and reservoir properties of oncolitic packstones, Macaé Formation (Albian–Cenomanian), Campos Basin, offshore Rio de Janeiro, Brazil. In T. M. Peryt (Ed.), Coated grains (pp. 330–343). Springer-Verlag. https://doi.org/10.1007/978-3-642-68869-0_28

Castro, R. D., & Picolini, J. P. (2016). Main features of the Campos Basin regional geology. In Geology and geomorphology (Vol. 1, pp. 1–12). Elsevier. https://doi.org/10.1016/B978-85-352-8444-7.50008-1

Catuneanu, O., Galloway, W. E., Kendall, C. G. S., Miall, A. D., Posamentier, H. W., Strasser, A., & Tucker, M. E. (2011). Sequence stratigraphy: Methodology and nomenclature. Newsletters on Stratigraphy, 44(3), 173–245. https://doi.org/10.1127/0078-0421/2011/0011

Chang, H. K., Kowsmann, R. O., Figueiredo, A. M. F., & Bender, A. (1992). Tectonics and stratigraphy of the East Brazil rift system: An overview. Tectonophysics, 213(1–2), 97–138. https://doi.org/10.1016/0040-1951(92)90253-3

Chiarella, D., & Longhitano, S. G. (2012). Distinguishing depositional environments in shallow-water mixed bio-siliciclastic deposits on the basis of the degree of heterolithic segregation (Gelasian, Southern Italy). Journal of Sedimentary Research, 82(12), 962–990. https://doi.org/10.2110/jsr.2012.78

Chiarella, D., Longhitano, S. G., & Tropeano, M. (2017). Types of mixing and heterogeneities in carbonate–siliciclastic sediments. Marine and Petroleum Geology, 88, 617–627. https://doi.org/10.1016/j.marpetgeo.2017.09.010

Chiarella, D., Moretti, M., Longhitano, S. G., & Muto, F. (2016). Deformed cross-stratified deposits in the Early Pleistocene tidally-dominated Catanzaro strait-fill succession, Calabrian Arc (Southern Italy): Triggering mechanisms and environmental significance. Sedimentary Geology, 344, 277–289. https://doi.org/10.1016/j.sedgeo.2016.05.003

Dahanayake, K. (1978). Sequential position and environmental significance of different types of oncoids. Sedimentary Geology, 20, 301–316. https://doi.org/10.1016/0037-0738(78)90060-X

De Ros, L. F., Goldberg, K., Abel, M., Victorinetti, F., Mastella, L., & Castro, E. (2007). Advanced acquisition and management of petrographic information from reservoir rocks using the PETROLEDGE® system. In AAPG Annual Conference and Exhibition. Long Beach, USA. Extended Abstracts, 6.

Dias-Brito, D., & Azevedo, R. L. M. (1986). As sequencias deposicionais marinhas da Bacia de Campos sob a otica paleoecologica. In Anais do 34° Congresso Brasileiro de Geologia (Vol. 1, pp. 38–49).

Dias, J. L., Scarton, J. C., Esteves, F. R., Carminatti, M., & Guardado, L. R. (1990). Aspectos da evolução tectono-sedimentar e a ocorrência de hidrocarbonetos na Bacia de Campos. In G. P. R. Gabaglia & E. J. Milani (Eds.), Origem e evolução de bacias sedimentares (pp. 333–360). Censud.

Dias, J. L., Vieira, J. C., Catto, A. J., Oliveira, J. Q., Guazeli, W., Trindade, L. A. F., Kowsmann, R. O., Kiang, C. H., Mello, U. T., Mizusaki, A. M. P., & Moura, J. A. (1987). Estudo regional da Formação Lagoa Feia. Petrobras/Depex, Relatório Interno.

Dickson, J. A. D. (1965). A modified staining technique for carbonates in thin section. Nature, 205, 587. https://doi.org/10.1038/205587a0

Dumas, S., Arnott, R. W., & Southard, J. B. (2005). Experiments on oscillatory-flow and combined-flow bedforms: Implications for interpreting parts of the shallow-marine sedimentary record. Journal of Sedimentary Research, 75(3), 501–513. https://doi.org/10.2110/jsr.2005.039

Favoreto, J., Rohn, R., Lykawka, R., Okubo, J., & Dias-Brito, D. (2015). Depositional, diagenetic and stratigraphic aspects of Macaé Group carbonates (Albian): Example from an oilfield from Campos Basin. Brazilian Journal of Geology, 45(2), 243–258. https://doi.org/10.1590/23174889201500020005

Ferronatto, J. P. F., Scherer, C. M. S., Drago, G. B., Rodrigues, A. G., Souza, E. G., Reis, A. D., Bállico, M. B., Kifumbi, C., & Cazarin, C. L. (2021). Mixed carbonate-siliciclastic sedimentation in a Mesoproterozoic storm-dominated ramp: Depositional processes and stromatolite development. Precambrian Research, 361, 106240. https://doi.org/10.1016/j.precamres.2021.106240

Figueiredo, A. M. F., & Mohriak, W. U. (1984). A tectonica salífera e as acumulaçoes de petroleo da Bacia de Campos. XXXIII Congresso Brasileiro de Geologia, Sociedade Brasileira de Geologia, 1380–1394.

Guardado, L. R., Gamboa, L. A. P., & Lucchesi, C. F. (1989). Petroleum geology of Campos Basin, Brazil: A model for producing Atlantic type basin. In J. D. Edwards & P. A. Santagrossi (Eds.), Divergent/Passive Margins Basins (AAPG Memoir 48, pp. 3–36). https://doi.org/10.1306/M48508C1

Guardado, L. R., Spadini, A. R., Brandão, J. S. L., & Mello, M. R. (2000). Petroleum system of the Campos Basin, Brazil. In M. R. Mello & B. J. Katz (Eds.), Petroleum Systems of South Atlantic Margins (AAPG Memoir 73, pp. 317–324). https://doi.org/10.1306/M73705C22

Gischler, E., & Lomando, A. J. (2005). Offshore sedimentary facies of a modern carbonate ramp, Kuwait, northwestern Arabian-Persian Gulf. Facies, 50, 443–462. https://doi.org/10.1007/s10347-004-0027-4

Grabau, A. W. (1904). On the classification of sedimentary rocks. Am. Geologist, 33, 228–247.

Koutsoukos, E. A. M. (1984). Evolucao paleoecologica do Albiano ao Maestrichtiano na area noroeste da Bacia de Campos, Brasil, com base em foraminíferos. 33 Congresso Brasileiro de Geologia, 2, 685–6.

McNeill, D. F., Cunningham, K. J., Guertin, L. A., & Anselmetti, F. S. (2004). Depositional themes of mixed carbonate-siliciclastics in the south Florida Neogene: Application to ancient deposits. In Integration of outcrop and modern analogs in reservoir modeling (AAPG Memoir 80, pp. 23–43).

McNeill, D. F., Klaus, J. S., Budd, A. F., Lutz, B. P., & Ishman, S. E. (2012). Late Neogene chronology and sequence stratigraphy of mixed carbonate-siliciclastic deposits of the Cibao Basin, Dominican Republic. Geological Society of America Bulletin, 124, 35–58. https://doi.org/10.1130/B30391.1

Miall, A. D. (1978). Lithofacies types and vertical profile models in braided river deposits: A summary. In A. D. Miall (Ed.), Fluvial Sedimentology (Canadian Society of Petroleum Geologists, Special Publication 5, pp. 587–604).

Michel, J., Mateu-Vicens, G., & Westphal, H. (2011). Modern heterozoan carbonate facies from a eutrophic tropical shelf (Mauritania). Journal of Sedimentary Research, 81, 641–655. https://doi.org/10.2110/jsr.2011.53

Mizusaki, A. M. P., Thomaz-Filho, A., & Cesero, P. (1998). Ages of the magmatism and the opening of the South Atlantic Ocean. Pesquisas, 25(2), 47–57. https://doi.org/10.22456/1807-9806.21166

Moretti, M., Tropeano, M., van Loon, A. J., Acquafredda, P., Baldacconi, R., Festa, V., Lisco, S., Mastronuzzi, G., Moretti, V., & Scotti, R. (2016). Texture and composition of the Rosa Marina beach sands (Adriatic coast, southern Italy): A sedimentological/ecological approach. Geologos, 22, 87–103. https://doi.org/10.1515/logos-2016-0011

Mount, J. F. (1984). Mixing of siliciclastic and carbonate sediments in shallow shelf environments. Geology, 12, 432–435. https://doi.org/10.1130/0091-7613(1984)12<432:MOSACS>2.0.CO;2

Okubo, J., Lykawka, R., Warren, L. V., Favoreto, J., & Dias-Brito, D. (2015). Depositional, diagenetic and stratigraphic aspects of Macaé Group carbonates (Albian): Example from an oilfield from Campos Basin. Brazilian Journal of Geology, 45(2), 243–258. https://doi.org/10.1590/23174889201500020005

Quirk, D. G., Schødt, N., Lassen, B., Ings, S. J., Hsu, D., Hirsch, K. K., & Von Nicolai, C. (2012). Salt tectonics on passive margins: Examples from Santos, Campos and Kwanza basins. Geological Society, London, Special Publications, 363, 207–244. https://doi.org/10.1144/SP363.10

Rebelo, T. B., Batezelli, A., & Luna, J. S. (2021). Stratigraphic evolution and carbonate factory implications: Case study of the Albian carbonates of the Campos Basin, Brazil. The Depositional Record, 7, 271–293. https://doi.org/10.1002/dep2.118

Rodrigues, R., & Takaki, T. (1987). Cretaceo Inferior nas bacias sedimentares da costa sudeste do Brasil-analise isotópica suas implicacoes paleoambientais. Revista Brasileira de Geociencias, 17, 177–179.

Rossi, V. M., Longhitano, S. G., Mellere, D., Dalrymple, R. W., Steel, R. J., Chiarella, D., & Olariu, C. (2017). Interplay of tidal and fluvial processes in an early Pleistocene, delta-fed, strait margin (Calabria, Southern Italy). Marine and Petroleum Geology, 87, 14–30. https://doi.org/10.1016/j.marpetgeo.2017.02.021

Schwarz, E., Veiga, G. D., Álvarez-Trentini, G., & Spalletti, L. A. (2016). Climatically versus eustatically controlled, sediment-supply-driven cycles: Carbonate-siliciclastic, high-frequency sequences in the Valanginian of the Neuquén Basin (Argentina). Journal of Sedimentary Research, 86, 312–335. https://doi.org/10.2110/jsr.2016.21

Schwarz, E., Veiga, G. D., Álvarez Trentini, G., Isla, M. F., & Spalletti, L. A. (2018). Expanding the spectrum of shallow-marine, mixed carbonate-siliciclastic systems: Processes, facies distribution and depositional controls of a siliciclastic-dominated example. Sedimentology, 65(5), 1558–1589. https://doi.org/10.1111/sed.12438

Simone, L. (1980). Ooids: A review. Earth Science Review, 16, 319–355. https://doi.org/10.1016/0012-8252(80)90053-7

Spadini, A. R., Esteves, F. R., Dias-Brito, D., Azevedo, R. L. M., & Rodrigues, R. (1988). The Macaé formation, Campos Basin, Brazil: Its evolution in the context of the initial history of the South Atlantic. Revista Brasileira de Geociencias, 18, 261–272.

Spadini, A. R. (1992). Processos deposicionais e ciclicidade em carbonatos albianos da plataforma rasa da Bacia de Campos (Master's thesis). Instituto de Geociências, Universidade Federal do Rio de Janeiro, Brazil.

Szatmari, P. (2000). Habitat of petroleum along the South Atlantic margins. In M. R. Mello & B. J. Katz (Eds.), Petroleum Systems of South Atlantic Margins (AAPG Memoir 73, pp. 69–75).

Thrana, C., & Talbot, M. R. (2006). High-frequency carbonate-siliciclastic cycles in the Miocene of the Lorca Basin (Western Mediterranean, SE Spain). Geologica Acta, 3, 343–354. https://doi.org/10.1344/105.000000348

Tanavsuu-Milkeviciene, K., Plink-Björklund, P., Kirsimäe, K., & Ainsaar, L. (2009). Coeval versus reciprocal mixed carbonate-siliciclastic deposition, Middle Devonian Baltic Basin, Eastern Europe: Implications from the regional tectonic development. Sedimentology, 56, 1250–1274. https://doi.org/10.1111/j.1365-3091.2008.01032.x

Tirsgaard, H. (1996). Cyclic sedimentation of carbonate and siliciclastic deposits on a late Precambrian ramp: The Elisabeth Bjerg Formations (Eleonore bay Supergroup), east Greenland. Journal of Sedimentary Research, 66, 699–712. https://doi.org/10.1306/D42683E7-2B26-11D7-8648000102C1865D

Veeken, P. C. H., & Moerkerken, B. van. (2013). Depositional environment and lithofacies interpretation. In Seismic Stratigraphy and Depositional Facies Models (pp. 215–374). https://doi.org/10.1016/b978-0-12-411455-5.50004-8

Wilson, J. L. (1975). Carbonate Facies in Geologic History. Springer. https://doi.org/10.1007/978-1-4612-6383-8

Winter, W. R., Jahnert, R. J., & França, A. B. (2007). Bacia de Campos. Boletim de Geociências da Petrobras, 15(2), 511–529.

Zuffa, G. G. (1980). Hybrid arenites: Their composition and classification. Journal of Sedimentary Petrology, 50, 21–29. https://doi.org/10.1306/212F7950-2B24-11D7-8648000102C1865D

Zeller, M., Verwer, K., Eberli, G. P., Massaferro, J. L., Schwarz, E., & Spalletti, L. (2015). Depositional controls on mixed carbonate–siliciclastic cycles and sequences on gently inclined shelf profiles. Sedimentology, 62, 2009–2037. https://doi.org/10.1111/sed.12215Thomson, P.-R., Jefferd, M., Clark, B.L., Chiarella, D., Mitchell, T.M., & Hier-Majumder, S. (2020b). Pore network analysis of Brae Formation sandstone, North Sea. Marine and Petroleum Geology, 122, 104614. https://doi.org/10.1016/J.MARPETGEO.2020.104614

Varloteaux, C., Békri, S., & Adler, P.M. (2013a). Pore network modelling to determine the transport properties in presence of a reactive fluid: From pore to reservoir scale. Advances in Water Resources, 53, 87–100. https://doi.org/10.1016/J.ADVWATRES.2012.10.004

Varloteaux, C., Vu, M.T., Békri, S., & Adler, P.M. (2013b). Reactive transport in porous media: Pore-network model approach compared to pore-scale model. Physical Review E—Statistical, Nonlinear, and Soft Matter Physics, 87(2), 23010. https://doi.org/10.1103/PhysRevE.87.023010

Wei, N., Gill, M., Crandall, D., McIntyre, D., Wang, Y., Bruner, K., Li, X., & Bromhal, G. (2014). CO_2 flooding properties of Liujiagou sandstone: influence of sub-core scale structure

heterogeneity. Greenhouse Gases: Science and Technology, 4(3), 400–418. https://doi.org/10.1002/ghg.1407

Wei, Y., Jin, J., Zhou, W., Zhou, H., Lou, Q., Xiong, Z., & Long, W. (2021). A New Image Upscaling Method for Digital Rock Simulation of Conglomerate Reservoir. In 2021 IEEE 5th Information Technology, Networking, Electronic and Automation Control Conference (ITNEC), 494–498. https://doi.org/10.1109/ITNEC52019.2021.9587219

Wentworth, C.K. (1922). A Scale of Grade and Class Terms for Clastic Sediments. The Journal of Geology, 30(5), 377–392

Yu, H., Zhang, Y., Ma, Y., Lebedev, M., Ahmed, S., Xiaolong, S., Verrall, M., Squelch, A., & Iglauer, S. (2019). CO_2-Saturated Brine Injection Into Unconsolidated Sandstone: Implications for Carbon Geosequestration. Journal of Geophysical Research: Solid Earth, 124(11), 10823–10838. https://doi.org/10.1029/2018JB017100

Zhan, X., Schwartz, L.M., Nafi Toksöz, M., Smith, W.C., & Dale Morgan, F. (2010). Pore-scale modeling of electrical and fluid transport in Berea sandstone. Geophysics, 75(5), F134–F142. https://doi.org/10.1190/1.3463704

How to cite: Amarante, F. B. do, Scherer, C. M. dos S., Armelenti, G., De Ros, L. F., Alvarenga, R., Kuchle, J., Conceição, J. C., Drummond Alves, J. L., & Landau, L. (2024). Depositional model and sedimentation controls of a complex hybrid carbonate–siliciclastic ramp (Albian) – SW Campos Basin, Brazil. Sedimentologika, 2(2), 1-22. https://doi.org/10.57035/journals/sdk.2024.e22.1535